

Metazoan evolution of glutamate receptors reveals unreported phylogenetic groups and divergent lineage-specific events

David Ramos-Vicente^{1,2}, Jie Ji³, Esther Gratacòs-Batlle⁴, Gemma Gou^{1,2}, Rita Reig-Viader^{1,2}, Javier Luís^{1,2}, Demian Burguera⁵, Enrique Navas-Perez⁵, Jordi García-Fernández⁵, Pablo Fuentes-Prior⁶, Hector Escrivá⁷, Nerea Roher³, David Soto⁴, Àlex Bayés^{1,2*}

¹Molecular Physiology of the Synapse Laboratory, Biomedical Research Institute Sant Pau, Barcelona, Spain; ²Universitat Autònoma de Barcelona, Barcelona, Spain; ³Institute of Biotechnology and Biomedicine, Department of Cell Biology, Animal Physiology and Immunology, Universitat Autònoma de Barcelona, Barcelona, Spain; ⁴Neurophysiology Laboratory, Department of Biomedicine, Medical School, August Pi i Sunyer Biomedical Research Institute, Institute of Neurosciences, Universitat de Barcelona, Barcelona, Spain; ⁵Department of Genetics, School of Biology, Institut de Biomedicina, University of Barcelona, Barcelona, Spain; ⁶Molecular Bases of Disease, Biomedical Research Institute Sant Pau, Hospital de la Santa Creu i Sant Pau, Barcelona, Spain; ⁷Sorbonne Université, CNRS, Biologie Intégrative des Organismes Marins, Banyuls-sur-Mer, France

*For correspondence:
abayesp@santpau.cat

Competing interests: The authors declare that no competing interests exist.

Funding: See page 22

Received: 09 February 2018

Accepted: 20 November 2018

Published: 22 November 2018

Reviewing editor: Leon D Islas, Universidad Nacional Autónoma de México, Mexico

© Copyright Ramos-Vicente et al. This article is distributed under the terms of the [Creative Commons Attribution License](https://creativecommons.org/licenses/by-nc-nd/4.0/), which permits unrestricted use and redistribution provided that the original author and source are credited.

Abstract Glutamate receptors are divided in two unrelated families: ionotropic (iGluR), driving synaptic transmission, and metabotropic (mGluR), which modulate synaptic strength. The present classification of GluRs is based on vertebrate proteins and has remained unchanged for over two decades. Here we report an exhaustive phylogenetic study of GluRs in metazoans. Importantly, we demonstrate that GluRs have followed different evolutionary histories in separated animal lineages. Our analysis reveals that the present organization of iGluRs into six classes does not capture the full complexity of their evolution. Instead, we propose an organization into four subfamilies and ten classes, four of which have never been previously described. Furthermore, we report a sister class to mGluR classes I-III, class IV. We show that many unreported proteins are expressed in the nervous system, and that new Epsilon receptors form functional ligand-gated ion channels. We propose an updated classification of glutamate receptors that includes our findings.

DOI: <https://doi.org/10.7554/eLife.35774.001>

Introduction

Glutamate is the principal excitatory neurotransmitter in the central nervous system of animals (Fonnum, 1984; Danbolt, 2001; Pascual-Anaya and D'Aniello, 2006). It acts on two families of structurally unrelated receptors: ionotropic glutamate receptors (iGluRs), which are ligand-gated ion channels and G-protein coupled receptors (GPCRs), known as metabotropic glutamate receptors (mGluRs) (Sobolevsky et al., 2009; Conn and Pin, 1997). While fast excitatory neurotransmission is mediated by iGluRs, metabotropic receptors modulate synaptic transmission strength. iGluRs are formed by four subunits, which can be traced back to bacteria (Tikhonov and Magazanik, 2009).

eLife digest Nerve cells or neurons communicate with each other by releasing specific molecules in the gap between them, the synapses. The sending neuron passes on messages through packets of chemicals called neurotransmitters, which are picked up by the receiving cell with the help of receptors on its surface. Neurons use different neurotransmitters to send different messages, but one of the most common ones is glutamate.

There are two families of glutamate receptors: ionotropic receptors, which can open or close ion channels in response to neurotransmitters and control the transmission of a signal, and metabotropic receptors, which are linked to a specific protein and control the strength of signal.

Our understanding of these two receptor families comes from animals with backbones, known as vertebrates. But the receptors themselves are ancient. We can trace the first family back as far as bacteria and the second back to single-celled organisms like amoebas. Vertebrates have six classes of ionotropic and three classes of metabotropic glutamate receptor. But other multi-celled animals also have these receptors, so this picture may not be complete.

Here, Ramos-Vicente et al. mapped all major lineages of animals to reveal the evolutionary history of these receptors to find out if the receptor families became more complicated as brain power increased. The results showed that the glutamate receptors found in vertebrates are only a fraction of all the types that exist. In fact, before present-day animal groups emerged, the part of the genome that holds the ionotropic receptor genes duplicated three times. This formed four receptor subfamilies, and our ancestors had all of them. Across the animal kingdom, there are ten, not six, classes of ionotropic receptors and there is an extra class of metabotropic receptors. But only two subfamilies of ionotropic and three out of four metabotropic receptor classes are still present in vertebrates today.

The current classification of glutamate receptors centers around vertebrates, ignoring other animals. But this new data could change that. A better knowledge of these new receptors could aid neuroscientists in better understanding the nervous system. And, using this technique to study other families of proteins could reveal more missing links in evolution.

DOI: <https://doi.org/10.7554/eLife.35774.002>

The current classification of iGluR subunits includes six classes: α -amino-3-hydroxy-5-methyl-4-isoxazolepropionic acid (AMPA) receptors, Kainate receptors, N-methyl-D-aspartate (NMDA) receptors (actually comprising three classes: NMDA1-3) and Delta receptors (Traynelis et al., 2010). iGluR subunits of the same class assemble into homo- or heterotetramers (Karakas and Furukawa, 2014; Kumar et al., 2011) and their ligand selectivity is dictated by a small number of residues located in the ligand-binding domain (Traynelis et al., 2010). Accordingly, NMDA subunits GluN1 and GluN3 as well as the Delta subunit GluD2 bind glycine and D-serine, while all subunits from the AMPA and Kainate classes bind glutamate (Traynelis et al., 2010; Kristensen et al., 2016). Metabotropic glutamate receptors are class C GPCRs and as such are formed by a single polypeptide. mGluRs also appeared before the emergence of metazoans, being present in unicellular organisms such as the amoeba *Dictyostellium discoideum* (Taniura et al., 2006). mGluRs are presently organized into three classes (I, II and III) and all their members respond to glutamate (Conn and Pin, 1997; Pin et al., 2003).

While the phylogeny of the two families of GluRs is well characterized in vertebrates, that of the entire animal kingdom is only poorly understood. The few studies on iGluR evolution outside vertebrates concentrate on a few phyla, leaving many proteins unclassified (Greer et al., 2017; Brockie et al., 2001; Janovjak et al., 2011; Kenny and Dearden, 2013). Similarly, the vast majority of mGluRs described so far fall into the three classes described in vertebrates (Krishnan et al., 2013; Kucharski et al., 2007; Dillon et al., 2006). Although, the existence of three insect mGluRs that cluster apart from classes I-III led to propose the existence of a fourth class (Mitri et al., 2004). Here we present what to our knowledge is the most comprehensive phylogenetic study of ionotropic and metabotropic GluRs along the animal kingdom. We have favored the use of more slow-evolving species for the construction of phylogenetic trees. These species are particularly amenable to phylogenetics (Simakov et al., 2013; Simakov et al., 2015; Putnam et al., 2007) as they arguably

present lower rates of molecular evolution than other organisms. Our work shows that metazoan evolution of GluRs is much more complex than previously thought. iGluRs present an overall organization into four subfamilies that were already present in the last ancestor of all metazoans. Vertebrate species only retain members of two of these subfamilies. Furthermore, we identify many lineage-specific gains, losses or expansions of GluR phylogenetic groups. Finally, we present experimental evidence showing that unreported GluRs found in the basally divergent chordate *Branchiostoma lanceolatum* (amphioxus) are highly expressed in the nervous system and that members of the unreported Epsilon subfamily, the most phylogenetically spread among unreported groups, can form functional ligand-gated ion channels.

Results

Phylogenetics of metazoan ionotropic glutamate receptors reveals four subfamilies, unreported classes and lineage-specific evolutionary dynamics

We have performed a systematic phylogenetic study of iGluR evolution across the animal kingdom. To increase the confidence on iGluRs evolutionary history phylogenetic trees have been generated using two independent methods (Bayesian inference and Maximum-likelihood (ML), **Figure 1** and **Figure 1—figure supplement 1**). Our analysis indicates that the family of iGluRs experienced key duplication events that define its present organization into four previously unreported subfamilies, of which two contain the extensively studied vertebrate classes. Assuming ctenophores as the sister group to all other animals (*Moroz et al., 2014; Ryan et al., 2013*), our data suggest that the three major duplication events leading to this four subfamilies occurred before the divergence of current animal phyla (see **Figure 2** for a summary scheme of iGluRs evolution). The first of these duplications produced the separation of the Lambda subfamily, the second lead to divergence of the NMDA subfamily and the third to the split between Epsilon and AKDF subfamilies.

The Lambda subfamily is the most phylogenetically restricted, as we could only identify it in porifers. Thus, Lambda would have been lost in two occasions, in the lineage of ctenophores and in a common ancestor of placozoans, cnidarians and bilaterals. On the other hand, the Epsilon subfamily is the best represented among non-bilaterians, being present in all non-bilaterian phyla investigated. Including in porifers, although we could only identify one Epsilon in sponges, GluE_Ifa from the demosponge *Ircinia fasciculata*. Our data also indicate that this subfamily has been lost in multiple occasions along metazoan evolution, as we could not find it in the protostome, echinoderm or vertebrate species investigated. Interestingly, all ctenophore iGluRs identified, which have been previously reported (*Alberstein et al., 2015*), belong to the Epsilon subfamily. Thus, this phylum would have lost NMDA, Lambda and AKDF proteins. Contrarily, ctenophores would have experienced an important expansion of Epsilon iGluRs, as we report 17 and 10 of these proteins in the two species with genomic information available, *M. leidy* and *P. bachei*, respectively.

Although we have not identified NMDA receptors in ctenophores, porifers and placozoans our analysis indicates that this subfamily was already present in the last common ancestor of metazoans. This is because the topology of the tree shows that NMDAs appear in the phylogeny at the same level as the Epsilon subfamily, which has representatives in all non-bilateral phyla. According to our data, NMDA1s on the one hand and NMDA2s and NMDA3s on the other contain members of the cnidarian phylum. Although we have only been able to identify one member more closely related to NMDA2 and NMDA3 than NMDA1 (GluN2/3_Nve), its position in the phylogeny is very well supported by both analyses performed. This indicates that a specific duplication occurred in the ancestor of bilaterians originating NMDA2s and NMDA3s. Moreover, we have also identified a cnidarian-specific NMDA class, that we have termed NMDA-Cnidaria, this class presents representative proteins in 3 of the four species investigated. Among bilaterals we have observed conservation of all NMDA classes with the exception of NMDA2s in echinoderms, which are absent from the two species examined. Interestingly, studied cnidarian species substantially expanded their NMDA subfamily repertoire, with at least six members in *Nematostella vectensis*.

In bilaterians the AKDF subfamily diversified into the known AMPA, Kainate and Delta classes, but also into a fourth new class that we have termed Phi. The phylogenetic spread of these classes is quite variable, as AMPA and Kainate are in all bilateral phyla investigated but Delta and Phi are

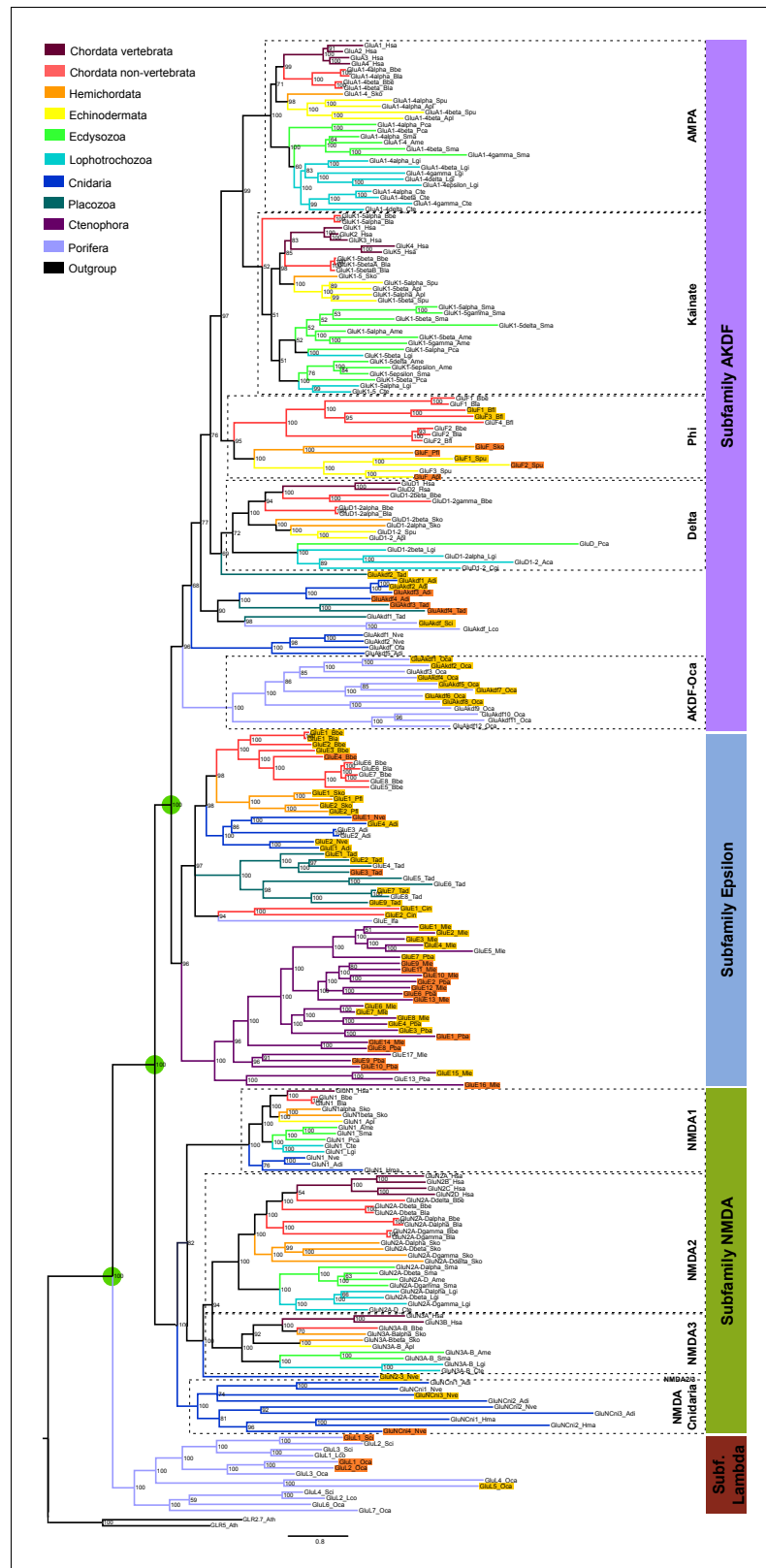


Figure 1. Bayesian phylogeny of metazoan ionotropic glutamate receptors. Ionotropic glutamate receptor subfamilies are indicated in colored boxes at the right. Sequences belonging to the same class are highlighted together by dashed lines and the class name is also shown. Green circles highlight the three duplications occurred before the divergence of the ctenophore lineage that lead to these four subfamilies. Posterior probabilities are *Figure 1 continued on next page*

Figure 1 continued

shown at tree nodes and protein names at the end of each branch. Tree branches are colored based on phylum, as indicated in the legend. For unreported phylogenetic groups, names of proteins predicted to bind glycine or glutamate are highlighted in yellow or orange, respectively. Protein names from non-vertebrate species are composed of four parts: (i) 'GluR#', where # is a code denoting class or subfamily (A, AMPA; K, Kainate; F, Phi; D, Delta; Akdf, AKDF; E, Epsilon; N, NMDA and L, Lambda); (ii) a number, or range of numbers, denoting orthologous vertebrate protein(s), if any; (iii) a Greek letter to identify non-vertebrate paralogs, if any and (iv) a three-letter species code. iGluRs from *A. thaliana* were used as an outgroup. All information on species and proteins used is given in **Figure 1—source data 2**. Phylogenetic reconstruction was performed using Bayesian inference. The amino acid substitution model used was Vt + G + F, number of generations: 14269000, final standard deviation: 0.007016 and potential scale reduction factor (PSRF): 1.000. Scale bar denotes number of amino acid substitutions per site. Although the GluAkdf2_Tad protein localizes to the Delta class in this tree, we do not consider this molecule as a confident member of this class. This is because the statistical support provided by the Bayesian analysis is low and because the Maximum-likelihood analysis (see **Figure 1—figure supplement 1**) does not position this protein in the Delta branch.

DOI: <https://doi.org/10.7554/eLife.35774.003>

The following source data and figure supplements are available for figure 1:

Source data 1. Conservation of protein domains in ionotropic glutamate receptors from unreported groups.

DOI: <https://doi.org/10.7554/eLife.35774.009>

Source data 2. Reference table of species and proteins used in the phylogenetic analysis of iGluRs.

DOI: <https://doi.org/10.7554/eLife.35774.010>

Source data 3. Aligned protein sequences used to construct ionotropic glutamate receptor phylogenies.

DOI: <https://doi.org/10.7554/eLife.35774.011>

Source data 4. Table with MolProbity scores of 3D models.

DOI: <https://doi.org/10.7554/eLife.35774.012>

Figure supplement 1. Maximum-likelihood phylogeny of metazoan ionotropic glutamate receptors.

DOI: <https://doi.org/10.7554/eLife.35774.004>

Figure supplement 2. Multiple protein alignment of transmembrane regions M1, M3 and M4 from unreported iGluRs.

DOI: <https://doi.org/10.7554/eLife.35774.005>

Figure supplement 3. Three-dimensional models of Epsilon class members.

DOI: <https://doi.org/10.7554/eLife.35774.006>

Figure supplement 4. Multiple protein alignment of the M1-M2 intracellular loop and the Q/R and +4 sites.

DOI: <https://doi.org/10.7554/eLife.35774.007>

Figure supplement 5. Multiple protein alignment of iGluR residues involved in ligand-binding.

DOI: <https://doi.org/10.7554/eLife.35774.008>

more restricted. Deltas are almost completely absent from ecdysozoan species, as we could only find a single member of this class in priapulids (*P. caudatus*) and none in arthropods or nematodes. Similarly, Deltas are poorly represented in mollusks and, with the available data, absent in annelids. Finally, we could only identify Phi proteins in cephalochordates, hemichordates and echinoderms, indicating that this class might be lost in the lineages of protostomes and outgroups (i.e. vertebrates and urochordates). The AKDF subfamily also includes proteins from the non-bilateral phyla of porifera, placozoa and cnidarian. The exact organization of these proteins into classes is not as straightforward as for bilateral proteins. The Bayesian and ML analysis only agree in the position of 12 iGluRs from the sponge *O. carmela*, these would constitute the only clear class in non-bilaterals, which we have termed AKDF-Oca.

Another example of a multiple lineage-specific event that occurred during animal evolution of iGluRs can be observed in the evolution of AMPA and Kainate proteins among protostomes. The general iGluRs phylogeny (**Figure 1**) suggests that ecdysozoan species have expanded their repertoire of Kainate subunits when compared with lophotrochozoans (e.g. mollusks, annelids), since *C. teleta* and *L. gigantea* only presents one and two genes coding for Kainate receptors, respectively. Contrarily, we found more AMPA subunits in lophotrochozoans than in ecdysozoan species. To investigate whether the two protostome lineages have alternatively expanded genes coding for AMPA or Kainate subunits we conducted a phylogenetic analysis of these two classes using eight species of ecdysozoans and seven of lophotrochozoans with well-characterized genomes (**Figure 3**

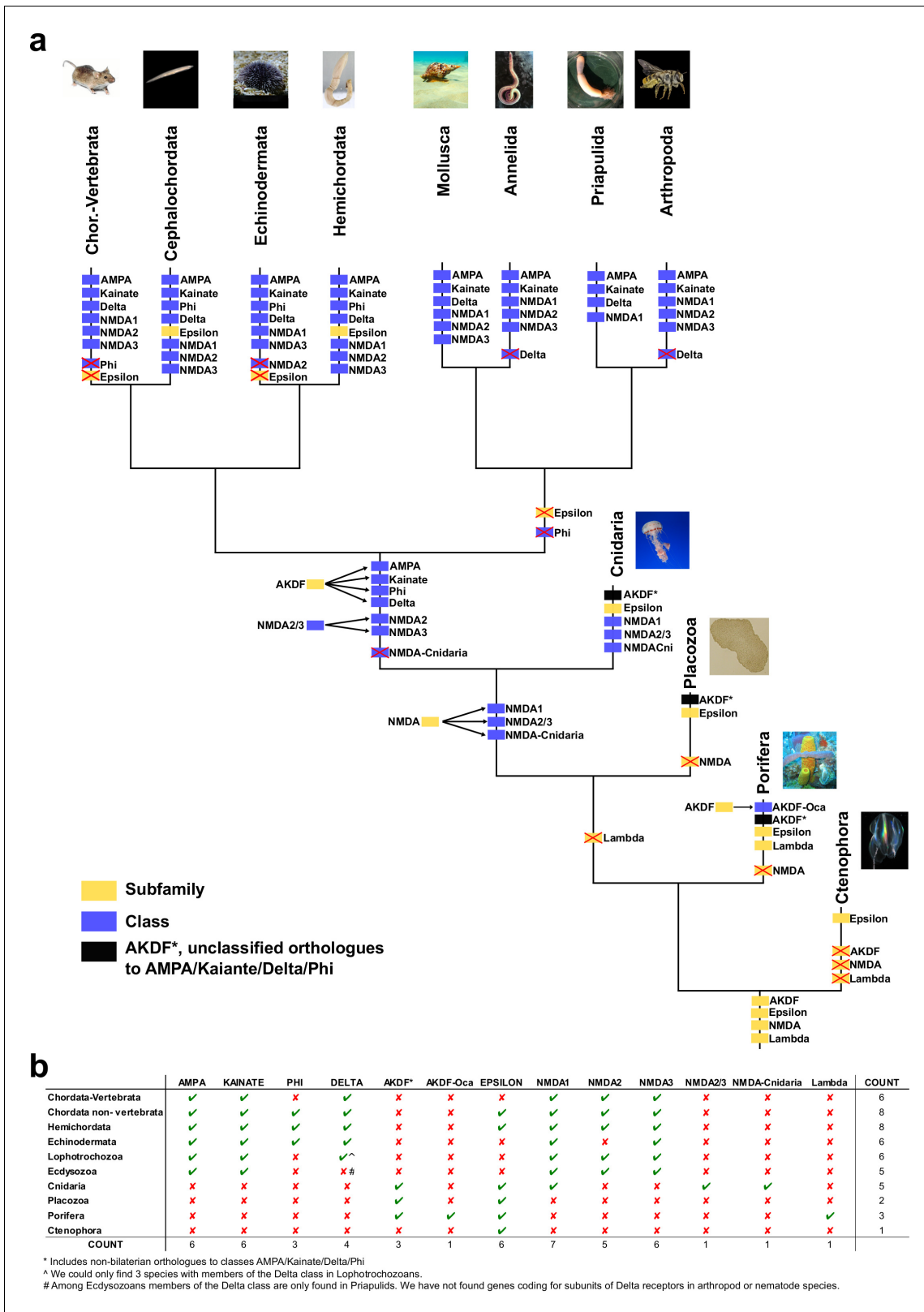


Figure 2. Schematic representation of iGluRs metazoan evolution. (a) Summary tree showing the evolution of iGluR subfamilies and classes in the metazoan lineages investigated. Each branch corresponds with one lineage. Phylogenetic subfamilies are represented by yellow boxes and classes by blue boxes. The four subfamilies present in the ancestor of all current metazoan lineages are shown at the base of the tree. Duplications of subfamilies in ancestors of current lineages are indicated. When a class or subfamily is lost in a lineage or in an ancestor, the corresponding box is crossed out with an orange 'X'. (b) Table showing the presence of subfamilies and classes in various metazoan groups. *Figure 2 continued on next page*

Figure 2 continued

a red cross. Mollusca and annelida are lophotrochozoans and priapulida and arthropoda ecdysozoans. In priapulida NMDA2s and NMDA3s were not investigated. (b) Table indicating the presence or absence of iGluR subfamilies and classes in the metazoan lineages investigated. When a phylogenetic group is present in a lineage it is indicated by a green tick and if it is absent by a red cross. The last column shows the total number of groups found in each phylum. The last row shows the number of phyla where each phylogenetic group is present.

Image credit: Placozoa, author Oliver Voigt, licensed under CC BY-SA 3.0 Germany license, source https://commons.wikimedia.org/wiki/File:Trichoplax_mic.jpg; *P. caudatus*, author Shunkina Ksenia, licensed under CC BY 3.0 source https://commons.wikimedia.org/wiki/File:Priapulidus_caudatus.jpg; Hemichordata, released under GNU Free Documentation License, source <https://commons.wikimedia.org/wiki/File:Eichelwurm.jpg>; Cephalochordata, author Hans Hillewaert, licensed CC BY-SA 4.0 International license, source https://commons.wikimedia.org/wiki/File:Branchiostoma_lanceolatum.jpg. DOI: <https://doi.org/10.7554/eLife.35774.013>

and **Figure 3—figure supplement 1**). Nematodes were left out of the analysis as they lack Kainate receptors (**Brockie et al., 2001**). This analysis retrieved 40 lophotrochozoan genes coding for AMPA subunits but only 15 coding for Kainates. The opposite scenario was observed in the genomes of ecdysozoan species, with 10 AMAP and 40 Kainate proteins. Yet, among ecdysozoans the priapulid *P. caudatus* has two AMPA and two Kainate subunits, indicating that the expansion of Kainate receptors might be exclusive to arthropods. Overall the AMPA:Kainate ratio resulted to be around 1:4 in ecdysozoans and 4:1 in lophotrochozoans.

Sequence conservation and ligand specificity of unreported iGluR phylogenetic groups

All proteins from unreported groups (i.e. subfamilies and classes) present well-conserved sequences in iGluR domains, including transmembrane domains or residues involved in receptor tetramerization (**Figure 1—figure supplement 2** and **Figure 1—source data 1**). Three-dimensional (3D) models of two Epsilon subunits from amphioxus (GluE1 and GluE7) indicate that their general fold is well preserved (**Figure 1—figure supplement 3a**). The only noticeable distinction in proteins from these groups is an insertion in the intracellular loop between the first and second transmembrane domains in Epsilon proteins. This insertion is particularly distinct in ctenophore iGluRs, having been termed as the cysteine-rich loop (**Alberstein et al., 2015**) (**Figure 1—figure supplement 4**). We have also identified a sequence difference among Epsilon proteins. Ctenophore iGluRs have two cysteines that form a disulfide bond at loop 1 of the ligand binding domain (**Alberstein et al., 2015**), which are also present in NMDA proteins. Nevertheless, this element is absent from the remaining members of the Epsilon subfamily.

The 'SYTANLAAF' motif, essential for channel gating (**Traynelis et al., 2010**), is also well conserved in most sequences, in particular the second, fourth and fifth residues (**Figure 1—figure supplement 2**). Nevertheless, all members of the Lambda subfamily and some proteins of the Phi class present lower levels of conservation in this sequence. Whether these changes have a functional impact is something that will require further investigation. The Q/R site (Q586, residue numbering according to mature rat GluA2) and the acidic residue located four positions downstream D/E590 (**Figure 1—figure supplement 4**) are involved in calcium permeability and polyamine block of AMPA and Kainate receptors (**Bowie and Mayer, 1995; Koh et al., 1995; Kamboj et al., 1995**). Of these two positions the latter is much better conserved, especially outside ctenophores and the Lambda subfamily. We have identified an acidic residue at position 590 in 84 out of 122 iGluRs from unreported groups, including cnidarian NMDAs. Yet, only 1/3 of these proteins present a glutamine (Q) at position 586. This includes most AKDFs and Epsilon proteins from non-ctenophores, contrarily, none of the Phi subunits presents a Q586.

The key ligand binding residues involved in fixing the amino acid backbone (α -amino and α -carboxyl) are Arg485 and an acidic residue at position 705 (**Naur et al., 2007; Armstrong and Gouaux, 2000; Mayer, 2005; Furukawa et al., 2005; Yao et al., 2008**). These two positions are well conserved in 94 of the 122 proteins from unreported groups, suggesting that their endogenous ligand is an amino acid (see **Figure 1—figure supplement 3b** for a 3D representation of ligand binding by GluE1 and **Figure 1—figure supplement 5** for an alignment of iGluR residues involved in ligand binding). The residue changes found in the remaining 28 proteins would render them unable to bind an amino acid (**Figure 1—figure supplement 5**). This is particularly common among class Phi proteins from amphioxus and in NMDA-Cnidaria.

Figure 3 continued

paralogues, if any and (iv) a three-letter species code. GluN1s from *chordates* were used as an outgroup. All information on species and proteins used in this phylogeny is given in **Figure 3—source data 2**. Phylogenetic reconstruction was performed using Bayesian inference. The amino acid substitution model used was Vt + I + G, number of generations: 8868000, final standard deviation: 0.0072 and potential scale reduction factor (PSRF): 1.001. Scale bar denotes number of amino acid substitutions per site.

DOI: <https://doi.org/10.7554/eLife.35774.014>

The following source data and figure supplement are available for figure 3:

Source data 1. Aligned protein sequences used to construct AMPA and Kainate class phylogenies in protostomes.

DOI: <https://doi.org/10.7554/eLife.35774.016>

Source data 2. Reference table of species and proteins used in the phylogenetic analysis of AMPA and Kainate classes in protostomes.

DOI: <https://doi.org/10.7554/eLife.35774.017>

Figure supplement 1. Maximum-likelihood phylogeny of AMPA and Kainate classes in protostomes.

DOI: <https://doi.org/10.7554/eLife.35774.015>

Residues involved in ligand selectivity show higher variability. These are located at positions 653 and 655, and are occupied by glycine and threonine in glutamate-binding proteins and by serine and a non-polar residue in glycine-binding iGluRs. However, a recent study of ctenophore receptors has found that position 653 can be occupied by serine or threonine in glutamate-binding iGluRs, and by an arginine in glycine-binding subunits (*Alberstein et al., 2015*). Based on this previous knowledge we have predicted the ligand specificities of most previously unreported receptors. The preferred ligand could be confidently predicted for 72 out of the 94 proteins with well-conserved residues involved in fixing the amino acid backbone.

Interestingly, all unreported groups comprise glycine- and glutamate-specific iGluRs. Gly-specific receptors slightly outnumber those predicted to respond to glutamate (overall ratio about 3:2). The Lambda subfamily would include three proteins specific for glutamate and one for glycine, while seven remain with an unknown selectivity. Of note, the protein predicted to bind glycine (GluL5_Oca) displays an arginine at position 653, a feature which had only been reported in ctenophores (*Alberstein et al., 2015*). This residue would form a salt bridge with Glu423, which is key for glycine selectivity in ctenophores (*Alberstein et al., 2015*). Most Epsilon and AKDF proteins would preferably bind glycine, although ctenophores present a similar number of Epsilon receptors predicted to respond to glycine or glutamate (**Figure 1**) (*Alberstein et al., 2015*). In the Phi class we also found a similar number of receptors binding glycine and glutamate. Finally, we could only predict binding specificity for two of the 9 NMDA-Cnidaria proteins, as they present many changes in the residues involved in either amino acid backbone binding or side chain recognition.

Interestingly, the 22 proteins for which we could not confidently predict their ligand selectivity (**Figure 1—figure supplement 5**), present a limited number of residues occupying position 653 and 655, suggesting constrained evolution. Of these: (i) nine present residues with negative polarity at both positions, being candidates to bind glutamate, (ii) six present a Gly653 and a non-polar residue at position 655, and thus are candidates to bind glycine, (iii) five proteins, all from the *Branchiostoma* genus, present a tyrosine at position 653. A structural model of one of these receptors, GluE7 (**Figure 1—figure supplement 3c**), shows that a Tyr653 aromatic side chain would occupy the ligand-binding pocket, strongly suggesting that amino acid binding would be blocked. Finally, (iv) two proteins present a phenylalanine in either of the two positions and remain unclassified.

Epsilon and Phi iGluR proteins are highly expressed in the nervous system and traffic to the plasma membrane

We used quantitative PCR (qPCR) to investigate gene expression levels of all iGluR subunits identified in *B. lanceolatum*, including those from the Epsilon and Phi groups. All 24 *B. lanceolatum* iGluR subunits identified in silico were found expressed in amphioxus, with the exception of *Grie5* (**Figure 4a**). Furthermore, they all showed a significantly higher expression in the nerve cord as compared to the whole body, suggesting tissue-enriched expression. While we observed low expression levels for Epsilon genes coding for subunits with a tyrosine at position 653 (*Grie5-8*), which according to the 3D model would block the ligand-binding pocket, the expression of *Grif1-2*, also presenting the same tyrosine, reach much higher levels, comparable to those of subunits from the Kainate,

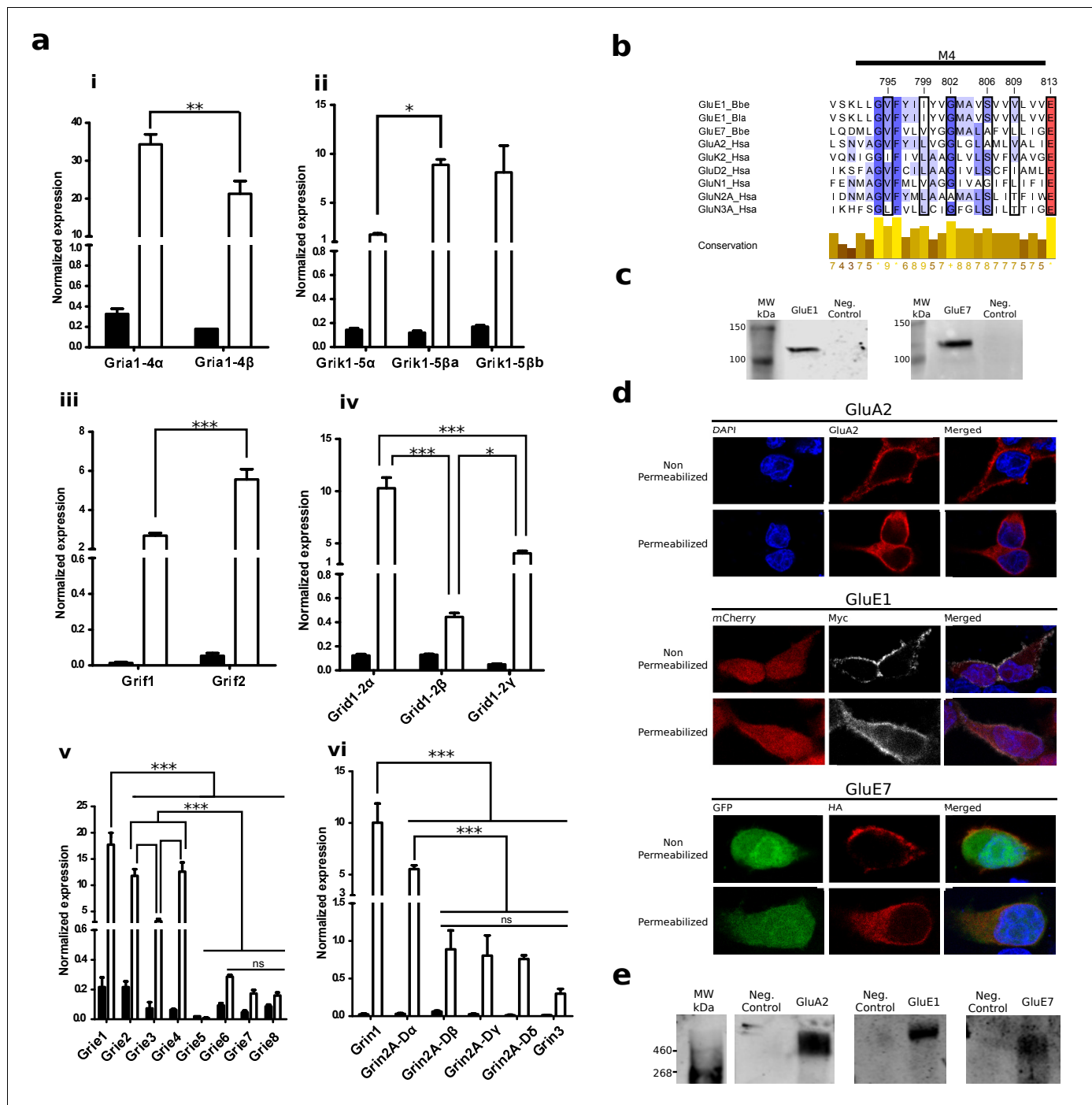


Figure 4. Expression and functional analysis of amphioxus iGluRs. (a) iGluRs mRNA expression (mean and standard deviation) in *Branchiostoma lanceolatum*. Bars show average relative expression of *B. lanceolatum* (amphioxus) iGluR genes as determined by qPCR. Filled bars represent whole body and open bars nerve cord expression levels. Note that all genes show significantly enriched expression in the nerve cord relative to the whole body, with the exception of *Grie5* (Student's t-test, $n = 3$). Expression level in the nerve cord is compared across genes of the same class. Statistics: pair comparisons were done by Student's t-test, $n = 3$, multiple comparisons were done by one-way ANOVA followed by Tukey's Post-Hoc test, $n = 3$. Significance levels: *** $p < 0.001$, ** $p < 0.01$ and * $p < 0.05$; ns, not significant. (i) AMPA class. (ii) Kainate class. (iii) Phi class. (iv) Delta class. (v) Epsilon subfamily. (vi) NMDA classes. (b) Multiple sequence alignment of iGluRs transmembrane region M4 containing residues involved in tetramerization, these are indicated by a black frame. Higher amino acid conservation is represented by increasing intensity of blue background and by a bar chart at the bottom. Sequences included are GluE1 and GluE7 from amphioxus and representatives of human iGluRs. (c) Immunoblot of chimeric GluE1 and GluE7, containing the signal peptide from rat GluA2, expressed in HEK293T cells. Proteins were detected using the immuno-tags (c-Myc and HA, respectively) located after the rat signal peptide. Protein extracts from non-transfected cells were loaded as negative controls. (d) Immunofluorescence

Figure 4 continued on next page

Figure 4 continued

of HEK293T cells expressing rat GluA2 (top), cMyc-tagged GluE1 (middle) or HA-tagged GluE7 (bottom). Both non-permeabilized and permeabilized conditions are shown. (e) Immunoblot of tetrameric rat GluA2, GluE1 and GluE7 expressed in HEK293T cells. Amphioxus proteins were detected using the immuno-tags (c-Myc and HA, respectively) located at the N-terminus of each sequence. Protein extracts from non-transfected cells were loaded as negative controls.

DOI: <https://doi.org/10.7554/eLife.35774.018>

The following source data and figure supplements are available for figure 4:

Source data 1. qPCR values used to generate **Figure 4a**.

DOI: <https://doi.org/10.7554/eLife.35774.021>

Figure supplement 1. Wild-type GluE1 and GluE7 expression in HEK293T cells and genetic strategy used to add a signal peptide.

DOI: <https://doi.org/10.7554/eLife.35774.019>

Figure supplement 2. List of primers used in qPCR experiments.

DOI: <https://doi.org/10.7554/eLife.35774.020>

Delta or NMDA classes. Thus, the presence of a tyrosine at position 653 does not appear to be directly correlated with low expression levels.

Amphioxus genes coding for GluE1 and GluE7 were synthesized in vitro and transiently expressed in HEK293T cells for functional studies. Wild-type GluE1 and GluE7, which are not predicted to have a canonical signal peptide by SignalP 4.1 (Nielsen, 2017), expressed well but were not trafficked to the plasma membrane (**Figure 4—figure supplement 1a–d**), even though residues involved in tetramerization (Salussolia et al., 2013) are well conserved (**Figure 4b**). We thus synthesized new variants of these genes with the signal peptide from rat GluA2 (**Figure 1—figure supplement 1cd**). These constructs also expressed well (**Figure 4c**) and now were efficiently trafficked to the plasma membrane, as indicated by the staining observed in non-permeabilized cells (**Figure 4d**). Furthermore, analysis of receptor oligomerization, performed using non-denaturing gel electrophoresis and immunoblot, clearly indicates that both proteins form homotetramers in vitro (**Figure 4e**).

Ligand specificity and electrophysiological properties of Epsilon proteins from amphioxus

We next investigated the gating properties of two Epsilon proteins from amphioxus, GluE1 and GluE7. The presence of a serine and a tryptophan at positions 653 and 704, respectively, suggested that GluE1 would bind glycine. Indeed, neither glutamate nor aspartate elicited a response in our experimental settings. Instead, glycine application was able to elicit an inward whole-cell current at a membrane potential of -60 mV (**Figure 5a**). Interestingly, the chemically related amino acids alanine and D-serine only generated very low responses, indicating a high selectivity of the GluE1 homotetramer for glycine.

The Epsilon receptor displayed a strong inward rectification, even in the absence of added polyamines in the intracellular solution (**Figure 5b,c**). This behavior is characteristic of unedited AMPA and Kainate receptors displaying a glutamine (Q) and an acidic residue at positions 586 and 590, respectively (Bowie and Mayer, 1995; Koh et al., 1995; Kamboj et al., 1995) and GluE1 presents a glutamine and an aspartic acid at these positions (**Figure 1—figure supplement 4**). Glycine-mediated currents showed a slow rate of recovery from desensitization when compared with AMPA or Kainate mammalian receptors, requiring 20–25 seconds until a complete recovery was achieved and a full response of the same magnitude could be recorded (**Figure 5d,e**). Similar observations have been made with ctenophore receptors activated by glycine in which the recovery from desensitization has an unusually long time constant of 81 seconds (Alberstein et al., 2015).

Finally, functional studies on receptors formed by GluE7 did not retrieve any positive results. None of the following amino acids: glutamate, aspartate, asparagine, glycine, alanine or D-serine elicited a response in our experimental system. We hypothesize that, as predicted by the 3D model, the presence of a tyrosine at position 653 renders a homomeric form of this receptor unable to function as an amino acid-gated ion channel.

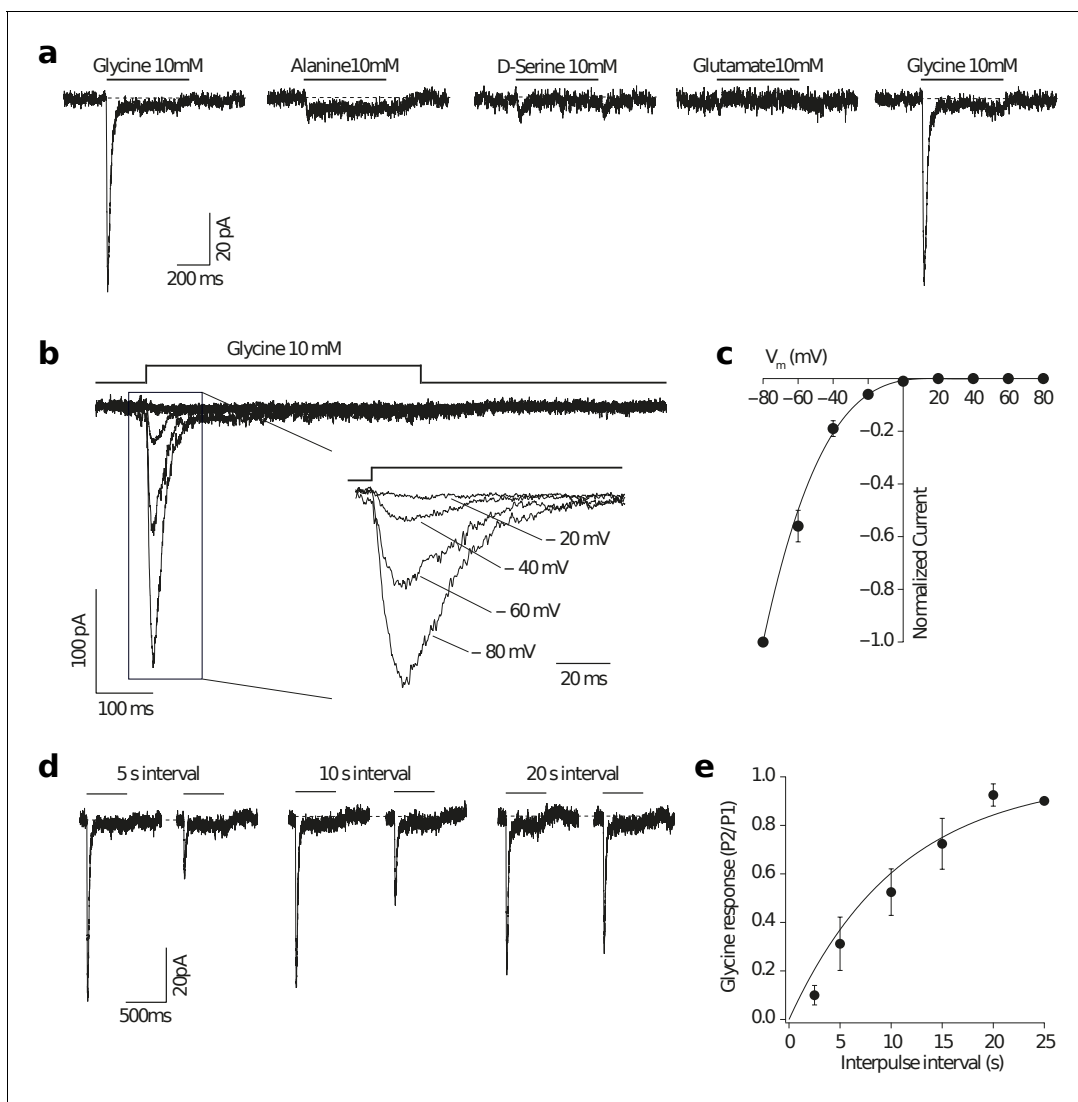


Figure 5. Glycine activates an amphioxus homomeric Epsilon receptor. (a) Representative homomeric GluE1 (from *B. lanceolatum*) whole-cell currents evoked by a rapid pulse (500 ms) of different amino acids (10 mM) in HEK293T cells. Left and right glycine-mediated currents denote agonist application before and after alanine, D-serine and glutamate applications respectively for ruling out run-down of the currents. (b) Representative GluE1 responses to 10 mM glycine at different membrane voltages (from -80 to $+80$ mV in 20 mV steps). Note that a strong inward rectification can be observed even in the absence of added polyamines in the intracellular solution. Inset: currents at negative membrane voltages are shown. (c) Current-voltage relationship for peak currents evoked by glycine (500 ms, 10 mM) applied to whole HEK293T cells containing homomeric GluE1 subunits normalized for the current at -80 mV ($n = 3$) fitted to a 5th order polynomial function. Error bars represent SEM. (d) Homomeric GluE1 glycine-mediated currents recorded at different time intervals by using a paired pulse protocol. (e) Rate of recovery of desensitization fitted to a single exponential of time constant 10.8 s ($n = 3-5$). Plot shows the average ratio values (P2/P1) and SEM (error bars).

DOI: <https://doi.org/10.7554/eLife.35774.022>

Phylogenetics of metazoan metabotropic glutamate receptors reveals a sister group of classes I to III

We next performed a phylogenetic study of metabotropic glutamate receptors (**Figure 6** and **Figure 6—figure supplement 1**). This analysis has revealed that the three historical mGluR classes (I to III) have a sister group. Following the current nomenclature we have named this as class IV. The existence of this class had already been proposed on the bases of three insect proteins (**Mitri et al., 2004**). Yet, here we show that this class is actually present in all bilateral phyla, excluding vertebrates. Furthermore, we also show that class IV appeared together with classes I-III before radiation of bilateral lineages. We have identified clear orthologues to class I-IV in porifers, placozoans and

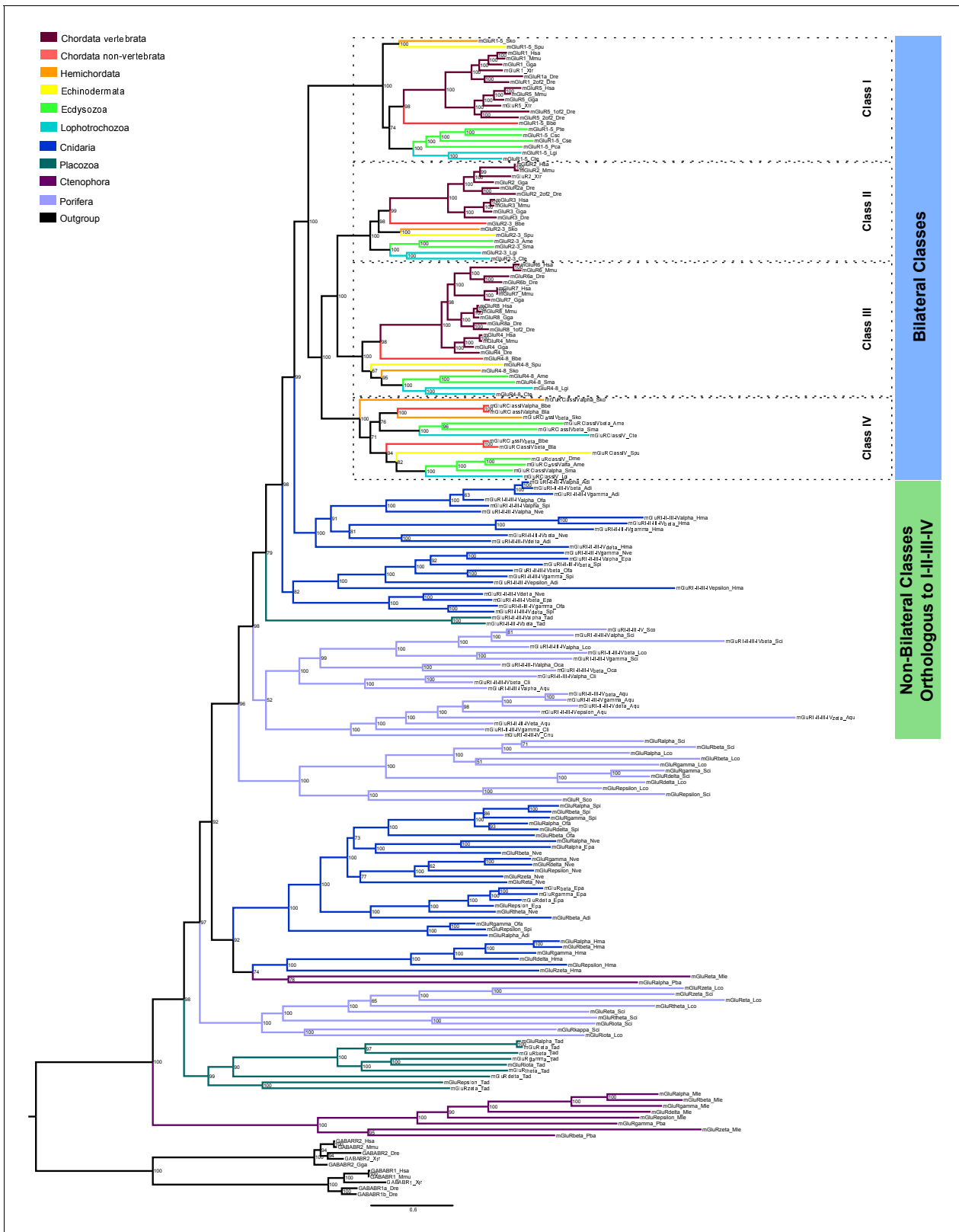


Figure 6. Bayesian phylogeny of metazoan metabotropic glutamate receptors. Identified metabotropic glutamate receptor classes from bilateral and non-bilateral organisms are indicated by colored boxes at the right. Dashed boxes further highlight individual classes from bilateral organism. Posterior probabilities are shown at tree nodes and protein names at the end of each branch. Tree branches are colored based on phylum, as indicated in the legend. Protein names from non-vertebrate species are composed of four parts: (i) 'mGluR', followed by a number, or range of numbers, denoting

Figure 6 continued on next page

Figure 6 continued

orthologous vertebrate protein(s), if any (for Class IV and group I-II-III-IV proteins, the name is followed by the name of the class/group); (ii) a Greek letter to identify non-vertebrate paralogs, if any and (iv) a three-letter species code. GABA-B receptors from vertebrates were used as an outgroup. All information on species and proteins used in this phylogeny is given in **Figure 6—source data 2**. Phylogenetic reconstruction was performed using Bayesian inference. The amino acid substitution model used was WAG + I + G + F, number of generations: 5327000, final standard deviation: 0.004788 and potential scale reduction factor (PSRF): 1.001. Scale bar denotes number of amino acid substitutions per site.

DOI: <https://doi.org/10.7554/eLife.35774.023>

The following source data and figure supplements are available for figure 6:

Source data 1. Conservation of protein domains in metabotropic glutamate receptors from unreported classes.

DOI: <https://doi.org/10.7554/eLife.35774.028>

Source data 2. Reference table of species and proteins used in the phylogenetic analysis of mGluRs.

DOI: <https://doi.org/10.7554/eLife.35774.029>

Source data 3. Aligned protein sequences used to construct metabotropic glutamate receptor phylogenies.

DOI: <https://doi.org/10.7554/eLife.35774.030>

Source data 4. qPCR values used to generate **Figure 6—figure supplement 2b**.

DOI: <https://doi.org/10.7554/eLife.35774.031>

Figure supplement 1. Maximum-likelihood phylogeny of metazoan metabotropic glutamate receptors.

DOI: <https://doi.org/10.7554/eLife.35774.024>

Figure supplement 2. Multiple protein alignment of mGluR residues involved in ligand binding and expression levels of *B.lanceolatum* mGluR genes.

DOI: <https://doi.org/10.7554/eLife.35774.025>

Figure supplement 3. Multiple protein alignment of mGluR transmembrane regions.

DOI: <https://doi.org/10.7554/eLife.35774.026>

Figure supplement 4. List of primers used in qPCR experiments.

DOI: <https://doi.org/10.7554/eLife.35774.027>

cnidarians but not in ctenophores. These are organized into four classes, two from cnidarians, and one from placozoans and porifers (**Figure 6**). We have also identified non-bilaterian mGluRs that fall outside the above-mentioned classes. Unfortunately, the Bayesian and ML phylogenies do not agree on the exact organization of these early divergent mGluRs, except for the fact that they diverge prior to bilaterian classes. For this reason we have left these sequences unclassified. Whether these sequences belong to one, or even multiple classes that would have been lost in bilateral organisms is something that will require further investigation.

Although all class IV proteins show well conserved sequences overall (**Figure 6—figure supplement 2a**, **Figure 6—figure supplement 3** and **Figure 6—source data 1**), two residues critical for glutamate binding, Arg78 and Lys409, are non-conservatively replaced by non-polar or acidic residues in all class IV proteins identified (**Figure 6—figure supplement 2a**, residue numbering corresponds to human mGluR1). These changes are predicted to hamper glutamate binding and, indeed, functional studies of a class IV receptor from fruit fly indicated that it does not respond to this amino acid (**Mitri et al., 2004**). All class IV proteins would share this feature. On the other hand, residues involved in contacts with the amino acid backbone are well conserved (**Figure 6—figure supplement 2a**), suggesting that these proteins might bind an amino acid other than glutamate. Similarly, mGluR residues from most non-bilaterian sequences involved in binding the amino acid backbone are highly conserved. Among non-bilaterian proteins the residues involved in glutamate binding are only conserved in approximately half of the proteins from classes orthologous to I-II-III-IV. Finally, we investigated mGluRs expression in amphioxus following the same procedure described for iGluRs. All five amphioxus mGluRs showed an enriched expression in the nerve cord, including the two class IV genes. Noticeably, these two genes showed significantly higher expression levels than orthologues of vertebrate classes (**Figure 6—figure supplement 2b**).

Discussion

We have performed what to our knowledge is the most comprehensive phylogenetic study of metazoan glutamate receptors. This has revealed that their evolutionary history is much more complex than what is currently acknowledged, especially for the family of iGluRs. Our study has also revealed the existence of unreported phylogenetic groups in both ionotropic and metabotropic glutamate

receptors. Importantly, our data indicate that the evolution of glutamate receptors has not occurred in an unequivocal incremental manner only in those clades with more elaborated neural systems, but it has rather followed a scattered lineage-specific evolutionary history. This means that certain lineages have experienced the gain, loss, expansion or reduction of specific phylogenetic groups.

Our phylogenetic analysis indicates that the family of iGluRs is actually divided into four unreported subfamilies that we have termed Lambda, Epsilon, NMDA and AKDF. Interestingly, this general organization was already present in the last common ancestor of all metazoans and later duplications within NMDA and AKDF subfamilies resulted in the formation of well-known iGluR classes. The other two subfamilies are absent from the majority of model species used in neuroscience research. The NMDA subfamily diversified into classes NMDA1-3 but also into the NMDA2/3 and NMDA-Cnidaria. Similarly, the AKDF subfamily diversified into the AMPA, Kainate and Delta classes, but also into the previously unreported Phi class. We have also identified an AKDF class exclusive to porifers, represented by sequences from *O. carmela*. Most well-studied iGluR classes are the result of duplications in ancestors of current bilateral species, >650 million years ago (mya) (Kumar et al., 2017), only class NMDA1 originated earlier, as cnidarians present members within this class. The Epsilon subfamily, which includes all iGluRs from ctenophores, is the only subfamily present in all non-bilateral phyla investigated, including sponges. It is thus the subfamily presenting a larger phylogenetic spread, as it is also present in hemichordates and in non-vertebrate chordates. On the other hand, the unreported Phi class shows a more restricted phylogenetic spread, as it is present only in three deuterostome phyla. Moreover, Lambda proteins seem restricted to Porifers, which constitutes an interesting evolutionary case due to maintenance of a glutamate receptor family in a phylum without nervous system.

The phylogenetic analysis of metabotropic glutamate receptors has allowed us to unambiguously establish the existence of a sister group to the well-known classes I, II and III. Following the present nomenclature we have named this as class IV. This class had been previously proposed based on the identification of three insect mGluRs that did not cluster with members of known classes (Mitri et al., 2004). Here we show that class IV is not restricted to insects, but is actually present in all bilaterian phyla investigated, with the exception of vertebrates where this class has been lost. Interestingly, as it occurs for most well-known iGluR classes, mGluR classes I-IV appeared simultaneously in the ancestor of bilaterals. Our phylogenetic analysis also indicates that the non-bilateral phyla of cnidarians, placozoans and porifers present clear orthologues to classes I-IV, which are organized into four classes, while we failed to find any in the early-branching ctenophores. Finally, we were unable to confidently classify many non-bilateral mGluRs, which might constitute one or more classes.

We have identified many examples of lineage-specific evolutionary events. These would antagonize with a model in which species with less elaborated nervous systems would present GluR families with lower complexity. The most noticeable examples are: (i) the absence of all subfamilies but Epsilon in analyzed ctenophores, (ii) the loss of Delta receptors from arthropods, nematodes and annelid species investigated, (iii) the loss of the Epsilon subfamily in vertebrates, echinoderms and protostomes, (iv) the loss of the Phi class in vertebrates and studied protostomes, (v) the specific expansion of Kainate receptors in arthropods, which contrasts with the expansion of AMPA receptors in its sister lineages of mollusks and annelids, (vi) the large expansion of the Epsilon subfamily in ctenophores, placozoans and cephalochordates and, finally (vii) the loss of mGluR class IV in vertebrates.

Along the same line, it is interesting to note that amphioxus (*B. belcheri* and *B. lanceolatum*), with a simple nervous system, have over 20 genes encoding iGluRs, while mammals have 18. Other non-vertebrate species also present large numbers of iGluRs, including the 19 iGluRs identified in the sponge *O. carmela* or the 17 present in the ctenophore *M. leidy*, to mention a few. Similarly, the cnidarian *A. digitifera* and the ctenophore *M. leidy* have seven mGluRs each, while the placozoan *T. adhaerens* presents eleven, three more than the eight mGluRs found in the human genome. The large number of GluRs found in many non-vertebrate animals suggests that there has been an evolutionary trend to increase their number in many metazoan lineages.

Our experimental results suggest that unreported receptors would play a role in the nervous system, as Epsilon, Phi and mGluR class IV genes are highly expressed in the nerve cord of amphioxus. Nevertheless, whether all these proteins are expressed at the synapse and act as neurotransmitter receptors is an issue that will require further investigation. Their presence in other tissues, such as sensory organs, cannot be ruled out. Those receptors showing more divergent sequences,

particularly in residues involved in ligand binding, might respond to other molecules. For instance, they could behave as chemoreceptors, as it is the case of antennal receptors found in insects (Croset *et al.*, 2010; Benton *et al.*, 2009).

Proteins from all unreported groups generally present a good conservation of residues involved in binding the amino acid backbone, indicating that their ligand would be an amino acid or a closely related molecule. Interestingly, we could identify proteins predicted to bind either glycine or glutamate in all unreported iGluR subfamilies and classes. If our functional predictions are correct, the ability to recognize one or the other amino acid would have emerged repeatedly in all unreported iGluR phylogenetic groups. Unexpectedly, the nature of the residues conferring amino acid specificity indicates that only a minority of proteins from unreported GluR groups would respond to glutamate. Sequence analysis and structural considerations strongly suggest that class IV mGluRs will not bind glutamate and that among non-bilateral mGluRs only a minority, belonging to classes orthologous to I-II-III-IV, are predicted to bind to this neurotransmitter. Similarly, among unreported iGluR groups, the number of proteins binding glycine outnumbers those binding glutamate. Interestingly, we report a glycine-binding poriferan protein (GluL5_Oca) with a structural feature that had only been reported in ctenophores (Alberstein *et al.*, 2015). This is an Arg653 that through establishing a salt bridge with Glu423 confers glycine specificity (Alberstein *et al.*, 2015). We thus report that this structural element is not exclusive to ctenophores. We have also identified iGluR subunits with important changes in critical ligand binding residues, indicating that they might have evolved new biological functions, for example, response to other, as yet unidentified small molecules.

The activation of Epsilon receptors by glycine has been experimentally corroborated by electrophysiological analysis of homotetrameric receptors composed by GluE7 from *M. leidy* (Alberstein *et al.*, 2015) and GluE1 from amphioxus (this study). In our hands the amphioxus receptor showed a very high selectivity for glycine, since ion currents could not be elicited by chemically related amino acids such as serine or alanine. Glycine-binding Epsilon subunits from phyla other than ctenophores present structural features similar to those from glycine-binding iGluRs in vertebrates. The greater number of glycine receptors found in non-vertebrate species could be related to the higher abundance of this amino acid in their nerve cord as compared with the mammalian brain (Pascual-Anaya and D'Aniello, 2006).

Altogether, our phylogenetic analysis and experimental findings have uncovered the complex evolution of glutamate receptors within the metazoan kingdom. Our data indicate that the classification of iGluRs is not restricted to the six classes currently recognized. Instead, iGluRs are organized into four subfamilies: Lambda, Epsilon, NMDA and AKDF and ten classes with varying phylogenetic spread. With the data available, the NMDA subfamily is organized into classes NMDA1, NMDA 2, NMDA3, NMDA-Cnidaria and NMDA2/3, while subfamily AKDF contains classes AMPA, Kainate, Delta, Phi and AKDF-Oca. Both NMDA2/3 and AKDF-Oca are represented by sequences from only one species, further sequencing of non-bilateral species will be required to fully demonstrate their existence. Furthermore, the evolution of mGluRs has generated a sister group to classes I, II and III, class IV. We have also identified classes of non-bilaterian mGluRs orthologous to I-II-III-IV. We propose that the classification of these two families of GluRs, key to the physiology of the nervous system, has to be updated to include our findings.

Materials and methods

Key resources table

Reagent type (species) or resource	Designation	Source or reference	Identifiers	Additional information
Cell line (<i>Homo sapiens</i>)	HEK293T	American Type Culture Collection	Cat#: CRL-3216 RRID: CVCL_0063	
Transfected construct (synthesize)	pIRES2_EGFP	Addgene	Cat. #: 6029–1	

Continued on next page

Continued

Reagent type (species) or resource	Designation	Source or reference	Identifiers	Additional information
Transfected construct (synthesize)	pCherryNeo	Addgene	Cat. #: 52119	
Transfected construct (synthesize)	<i>Grie1</i> in pCherryNeo	Invitrogen GeneArt Gene Synthesis		
Transfected construct (synthesize)	<i>Grie7</i> in pRES2_EGFP	Invitrogen GeneArt Gene Synthesis		
Biological sample (<i>Branchiostoma lanceolatum</i>)	whole animal			Collected in the bay of Argelès-sur-Mer, France (latitude 42° 32' 53' N and longitude 3° 03' 27' E)
Biological sample (<i>Branchiostoma lanceolatum</i>)	nerve chord			Collected in the bay of Argelès-sur-Mer, France (latitude 42° 32' 53' N and longitude 3° 03' 27' E)
Antibody	Mouse anti-HA	Covance	Cat. #: MMS-101P RRID: AB_291259	IF (1:200), WB (1:1000)
Antibody	Rabbit anti-c-Myc	Cell Signalling	Cat. #: 2272S RRID: AB_10692100	IF (1:100), WB (1:1000)
Antibody	Mouse anti-GluA2	Millipore	Cat. #: MAB397 RRID: AB_2113875	IF (1:200), WB (1:1000)
Antibody	Alexa Fluor 555 donkey anti-mouse IgG	Invitrogen	Cat. #: A-31570 RRID: AB_2536180	IF (1:1000)
Antibody	Alexa Fluor 647 goat anti-rabbit IgG	Life Technologies	Cat. #: A-21245 RRID: AB_2535813	IF (1:500)
Antibody	Donkey anti-mouse	Li-cor	Cat. #: 926-32212 RRID: AB_621847	WB (1:7500)
Antibody	Donkey anti-rabbit	Li-cor	Cat. #: 926-68073 RRID: AB_10954442	WB (1:7500)
Recombinant DNA reagent				
Sequence-based reagent	<i>Grie1</i> gene from <i>B. lanceolatum</i>			
Sequence-based reagent	<i>Grie7</i> gene from <i>B. Belcheri</i>			

Continued on next page

Continued

Reagent type (species) or resource	Designation	Source or reference	Identifiers	Additional information
Sequence-based reagent	Sequecne corresponding with rat <i>Gria2</i> signal peptide			
Chemical compound, drug	N-dodecyl- α -maltopyranoside; DDM	Anatrace	Cat. #: D310HA	2% w/v
Software, algorithm	pClamp10	Molecular Devices		
Software, algorithm	IgorPro	Wavemetrics		
Software, algorithm	Neuromatic	doi: 10.3389/fninf.2018.00014	RRID: SCR_004186	
Software, algorithm	MrBayes 3.2.6	doi: 10.1093/sysbio/sys029		
Software, algorithm	IQTree	doi: 10.1093/molbev/msu300		
Software, algorithm	MolProbity	doi: 10.1107/S0907444909042073	RRID: SCR_014226	
Software, algorithm	MIFit	GitHub (Smith, 2010)		
Software, algorithm	FIJI	doi: 10.1038/nmeth.2019	RRID: SCR_002285	
Other	CIPRES Science Gateway	doi: 10.1109/GCE.2010.5676129	RRID: SCR_008439	Free on-line super computing resource for evolutionary research

Identification of genes coding for members of glutamate receptor families in metazoan genomes

Phylogenetic analysis were performed with sequences from at least two species from each of the following metazoan phyla: Porifera, Ctenophora, Placozoa, Cnidaria, Lophotrochozoa, Ecdysozoa, Hemichordata, Chordata and Vertebrata, with the exception of placozoans for which only one species is available. When possible, we chose slowly evolving species. The complete lists of species used for iGluR phylogenies are given in **Figure 1—source data 2**. Species used in the phylogeny of metabotropic glutamate receptors are listed in **Figure 6—source data 2**. Sponge sequences were taken from ([Riesgo et al., 2014](#)), *B. lanceolatum* sequences were retrieved from unpublished genomic and transcriptomic databases (access was kindly provided by the Mediterranean Amphioxus Genome Consortium), *A. digitifera* and *P. flava* sequences were obtained from the Marine Genomics Unit ([Simakov et al., 2015](#); [Shinzato et al., 2011](#)) and *P. bachei* sequences from NeuroBase ([Moroz et al., 2014](#)).

GluR sequences were identified using homology-based searches in a two-tier approach. Mouse glutamate receptors were used as search queries (iGluRs: *Gria1-4*; *Grik1-5*; *Grid1-2*, *Grin1*, *Grin2A-D* and *Grin3A-B*; mGluRs: *mGluR1-8*). In a first search GluR homologs were identified using the BLASTP tool ([Altschul et al., 1990](#)) with default parameters. Subject sequences with an E-value below 0.05 were selected as candidate homologs. These were re-blasted against the NCBI database of 'non-redundant protein sequences' using the same BLAST tool. If the first hit obtained in the reciprocal BLAST was a glutamate receptor the sequence was included in the phylogenetic analysis. In a second stage the same mouse sequences were used to perform TBLASTN searches against

genomic and, when available, transcriptomic databases. Subject sequences not identified in the first run and having an E-value below 0.05 were selected as candidate homologs. These were re-blasted using BLASTX against the NCBI 'non-redundant protein sequences' database. Finally, if the first hit of this search was a glutamate receptor the sequence was also included in the phylogenetic analysis. Identified iGluR sequences in which less than four residues of the SYTANLAAF motif (Traynelis et al., 2010) were conserved were not considered for the final phylogenetic analysis. mGluR sequences lacking two or more of the seven transmembrane regions were also discarded. The complete reference lists of all iGluRs used in the final phylogeny are given in files **Figure 1—source data 2**. The reference list of metabotropic glutamate receptors is presented in **Figure 6—source data 2**. The alignments used for the phylogenetic analysis of iGluRs, mGluRs and AMPAs and Kainates from protostomes are provided in **Figure 1—source data 3**, **Figure 3—source data 1** and **Figure 6—source data 3**.

Phylogenetic analyses

The iGluR tree was constructed with 224 sequences identified in 26 non-vertebrate species (**Figure 1—source data 2**). The tree also included 18 iGluR sequences from vertebrates and two iGluR proteins from *A. thaliana*, used as an outgroup (Chiu et al., 2002). The phylogenetic analysis of AMPA and Kainate classes in protostomes was inferred using 110 sequences from 15 protostome species (**Figure 3—source data 2**) and 37 sequences from deuterostomes, of which 4 GluN1 proteins were used as an outgroup. The mGluR tree was constructed with 149 proteins from 29 non-vertebrate species, 38 mGluRs from vertebrate species and 10 sequences from vertebrate metabotropic GABA receptors, used as an outgroup (**Figure 6—source data 2**).

Protein sequences were aligned with the MUSCLE algorithm (Edgar, 2004), included in the software package MEGA6 (Tamura et al., 2013) with default parameters. ProtTest v3.4.2 was used to establish the best evolutionary model (Darriba et al., 2011). Trees were constructed using MrBayes v3.2.6 (Ronquist et al., 2012) for Bayesian inference and IQ-TREE (Nguyen et al., 2015) for Maximum-likelihood analysis. For Bayesian inference phylogenies were stopped when standard deviation was below 0.01 and its value was fluctuating but not decreasing. Markov chain Monte Carlo (MCMC) was used to approximate the posterior probability of the Bayesian trees. Bayesian analyses included two independent MCMC runs, each using four parallel chains composed of three heated and one cold chain. Twenty-five % of initial trees were discarded as burn-in. Convergence was assessed when potential scale reduction factor (PSRF) value was between 1.002 and 1.000. In Maximum-likelihood analysis the starting tree was estimated using a neighbor-joining method and branch support was obtained after 1000 iterations of ultrafast bootstrapping (Hoang et al., 2018). Gene/protein names were given based on their position in the tree. Phylogenetic trees were rendered using FigTree (<http://tree.bio.ed.ac.uk/software/figtree/>). Phylogenetic calculations were performed at the IBB - UAB heterogeneous computer cluster 'Celler' and at the CIPRES science gateway (RRID: SCR_008439) (Miller et al., 2010).

Collection and housing of animals

Branchiostoma lanceolatum adults were collected in the bay of Argelès-sur-Mer, France (latitude 42° 32' 53' N and longitude 3° 03' 27' E) with a specific permission delivered by the Prefect of Region Provence Alpes Côte d'Azur. *B. lanceolatum* is not a protected species. Animals were kept in tanks with seawater at 17°C under natural photoperiod.

RNA isolation, cDNA synthesis and quantitative gene expression (qPCR)

Adult amphioxus (*B. lanceolatum*) were anesthetized in 0.1% diethyl pyrocarbonate (DEPC; Sigma, D5758) PBS buffer. Animals were sacrificed by cutting the most anterior part of the body. The nerve chord was surgically extracted from the animal while submerged in DEPC-PBS using a magnifying glass. Individual nerve chords were snap frozen in liquid nitrogen and stored at -80°C until use. RNA was extracted from whole animals or from dissected nerve chords. Ten nerve chords were used for each RNA extraction, so that biological variability between individuals could be normalized. The tissue was homogenized in 1 mL of TRI Reagent (Sigma, T9424) using a Polytron homogenizer. Homogenates were transferred into an Eppendorf tube and incubated 5 min at room temperature

(RT) before adding 100 μL of 1-bromo-3-chloropropane. Tubes were vigorously mixed by vortexing for 10–15 s, incubated 15 min at RT and centrifuged at 13000 rpm for 15 min at 4°C. RNA was precipitated from the aqueous phase with 500 μL of isopropanol and 20 μg of glycogen. Tubes were frozen for 1 hr at -80°C and then thawed, incubated at RT for 10 min and centrifuged at 13000 rpm for 10 min at 4°C. The RNA pellet was washed twice with 500 μL of 75% ethanol and air-dried. cDNA was synthesized from 0.5 μg of total RNA. One μL of Oligo(dT)15 (Promega), 1 μL of 10 mM dNTP mix (Biotools), RNA and DEPC distilled water were mixed in a PCR tube to a final volume of 14 μL . This mix was incubated at 65°C for 5 min in a T100 Thermal Cycler (BioRad). After cooling tubes on ice for 1 min, we added 4 μL of First Strand 5x buffer, 1 μL of 0.1 M DTT and 1 μL of SuperScript III (Invitrogen). Tubes were placed in a T100 Thermal Cycler (BioRad) with the following program: 60 min at 50°C, 15 min at 70°C. RNA expression levels were determined using qPCR and the GAPDH gene used as a reference. Primers used for qPCR analysis of iGluRs are in **Figure 4—figure supplement 2** and those used for mGluR qPCR in **Figure 6—figure supplement 4**. qPCR data for iGluRs and mGluRs are given in **Figure 4—source data 1** and **Figure 6—source data 4**, respectively.

cDNA from nerve chord and whole body samples was diluted 1:10 for the glutamate receptor gene reactions, and 1:100 for the reference gene reaction. For each gene 2.5 μL of diluted cDNA were added to 5 μL of iTaq Universal SYBR Green Supermix (Bio-Rad), along with 0.5 μL of each primer and 1.5 μL of RNase free water. qPCR was run in a C1000 Touch thermocycler combined with the optic module CFX96. Three technical replicates were performed for all genes analyzed. Primer pairs were designed to detect the expression levels of each glutamate receptor (**Figure 4—figure supplement 2** and **Figure 6—figure supplement 4**). *B. belcheri* glutamate receptor sequences were aligned with the genomic sequence of *B. lanceolatum*, and high identity fragments were used to design primers. All primers were 20–25 base pair long, had GC content over 40–45% and a T_m between 60–65°C. Primers were designed to obtain amplicons between 140–270 base pairs. Values of normalized expression were statistically analyzed using GraphPad Prism5. No outliers were identified and no data points were excluded. Comparisons between whole body and nerve chord expression levels were done with Student's T-Test for unpaired samples or the Welch variant of the Student's T-Test for samples with different variance. For multiple comparisons between the expression levels of genes belonging to the same class one-way ANOVA analysis was performed using Tukey's Post-Hoc test.

Grie1 and Grie7 gene synthesis

Grie1 and *Grie7* genes were selected for transient expression in the mammalian cell line HEK293T. We prepared two constructs for each gene. We first introduced an immuno-tag in the N-terminus before the first element of secondary structure. For *Grie1* we used the c-Myc tag, which was placed after residue 39, and for *Grie7* we used the hemagglutinin (HA) tag introduced after residue 10 of the wild-type sequence. The second set of constructs prepared substituted the wild type N-terminal sequence for the signal peptide from rat GluA2 while maintaining the immuno-tags (**Figure 4—figure supplement 1**). Codon-optimized genes for expression in human cells were synthesized and cloned into pCherryNeo (Addgene, 52119) and pIRES2_EGFP (Addgene 6029–1) by the Invitrogen GeneArt Gene Synthesis service.

Cell line

All expression experiments were done with a mycoplasma-free HEK293T cell line kindly provided by Prof. F. Ciruela (Universitat de Barcelona) and purchased from the American Type Culture Collection (ATCC, CRL-3216, RRID: [CVCL_0063](https://doi.org/10.26434/chemrxiv-2019-06-01)). The ATCC has confirmed the identity of HEK293T by STR profiling (STR Profile; CSF1PO: 11,12; D13S317: 12,14; D16S539: 9,13; D5S818: 8,9; D7S820: 11; TH01: 7, 9.3; TPOX: 11; vWA: 16,19; Amelogenin: X). After the purchase of the cell line, mycoplasma tests are performed in the laboratory on every new defrosted aliquot. The kit used for mycoplasma detection is Plasmotest (Invivogen, code: rep-pt1).

Expression of GluE1 and GluE7 in HEK293T cells and analysis of plasma membrane trafficking

HEK293T cells were maintained in Dulbecco's Modified Eagle Medium (DMEM) supplemented with 10% FBS and 1% Antibiotic-Antimycotic (Gibco) in a humidified incubator at 5% CO₂ air and 37°C. The day before transfection, cells were plated onto poly-D-lysine coated coverslips in 6-well plates, to reach 60–80% confluence. HEK293T cells were transiently transfected with the following plasmids: empty pIRES2-EGFP, pIRES2-EGFP containing the *Grie7_Bbe* gene, empty pCherryNeo and pCherryNeo containing *Grie1_Bla*. Cells were transfected using 3 µg of polyethylenimine and 1 µg of plasmid DNA for each ml of non-supplemented DMEM. Cells were incubated 4–5 hr with transfection medium without supplementation, which was then removed and replaced by supplemented medium. Twenty-four hours after transfection the medium was removed and cells were washed 3 times with PBS. For surface receptor staining, cells were blocked in 2% BSA in PBS for 10 min at 37°C, and incubated for 25 min at 37°C with primary antibodies against HA (Covance, MMS-101P, RRID: [AB_291259](#)), c-Myc (Cell Signalling, 2272S, RRID: [AB_10692100](#)) or GluA2 (Millipore, MAB397, RRID: [AB_2113875](#)). HA and GluA2 antibodies were diluted 1:200 and c-Myc 1:100 in DMEM without supplementation. Cells were washed 3 times with PBS, fixed in 4% paraformaldehyde (PFA) for 15 min at RT, rinsed in PBS and incubated 1 hr at 37°C with secondary antibodies Alexa Fluor 555 donkey anti-mouse IgG (H + L) (A-31570, Invitrogen, RRID: [AB_2536180](#)) and Alexa Fluor 647 goat anti-rabbit IgG (H + L) highly cross-adsorbed (Life Technologies, A-21245, RRID: [AB_2535813](#)), diluted 1:1000 and 1:500 in PBS, respectively. Finally, coverslips were washed and mounted onto slides with Fluoroshield with DAPI (Sigma-Aldrich, F6057). For intracellular labeling cells were first fixed in 4% PFA for 15 min at RT, permeabilized with 0.2% Triton X-100 in PBS for 10 min, and finally blocked with PBS containing 2% BSA and 0.2% Triton X-100 for 20 min. Primary antibodies against HA (Covance, MMS-101P, RRID: [AB_291259](#)) and GluA2 (Millipore, MAB397, RRID: [AB_2113875](#)) were diluted 1:1000 and c-Myc (Cell Signalling, 2272S, RRID: [AB_10692100](#)) antibody was prepared at 1:100 in PBS. Incubation lasted 25 min at 37°C. Secondary antibody incubations and coverslip mounting were done in the same way as for non-permeabilized cells. Cells were examined using a confocal laser-scanning microscope (Zeiss LSM 700) with a 63x oil objective.

Western blot and native gel electrophoresis

HEK293T cells were grown in 6-well plates as described previously and transfected with plasmids expressing amphioxus GluE1, GluE7 or GluA2. Twenty-four hours after transfection cells were rinsed with PBS and the content of 4 wells was resuspended in solubilization buffer (PBS containing 2% N-dodecyl- α -maltopyranoside (DDM; D310HA, Anatrace) and the protease inhibitors mix cOmplete EDTA-free Protease Inhibitor Cocktail, Roche). Cell lysates were homogenized in a Dounce homogenizer in ice with 20 strokes and kept under orbital agitation for 1 hr at 4°C. Lysates were centrifuged at 89000xg in a Beckman TLA120.2 rotor for 40 min at 4°C. The supernatant containing solubilized membrane proteins was recovered in a new tube and stored at –20°C until used.

For native gel electrophoresis proteins were resolved in a Mini-PROTEAN TGX Gel 4–20% (Bio-Rad). Samples were mixed with Native Sample Buffer (Bio-Rad) and run along with HiMark Pre-Stained Protein Standard (Life Technologies). Electrophoresis was performed in ice at a constant voltage of 100 V for 180 min. Gels were transferred at constant current (35 mA) to polyvinylidene fluoride (PVDF) membranes overnight (16–18 hr) at 4°C. After transfer, membranes were blocked for 1 hr with Odyssey Blocking Buffer (Li-cor) in TBS, and incubated overnight at 4°C with primary antibodies anti-HA (Covance, MMS-101P, RRID: [AB_291259](#)), anti-c-Myc (Cell Signaling, 2272S, RRID: [AB_10692100](#)) or anti-GluA2 (Millipore, MAB397, RRID: [AB_2113875](#)) diluted 1:1000 in TTBS (TBS containing 0.05% Tween-20). After three 15 min washes in TTBS, membranes were incubated with donkey anti-mouse (Li-cor, 926–32212, RRID: [AB_621847](#)) and donkey anti-rabbit (Li-cor, 926–68073, RRID: [AB_10954442](#)) diluted 1:7500 in TTBS for 1 hr. Blots were analyzed in an Odyssey scanner (Li-cor).

For denaturing gel electrophoresis (SDS-PAGE) protein lysates were denatured by adding loading sample buffer 10x (500 mM Tris-HCl pH 7.4, 20% SDS, 10% β -mercaptoethanol, 10% glycerol and 0.04% bromophenol blue), and incubated for 5 min at 95°C. Protein lysates were loaded in a 10% SDS-polyacrylamide gel and separated at a constant current (25 mA). Gels were transferred at a constant voltage of 100 V for 90 min in ice. Membranes were blocked for 1 hr with Odyssey Blocking

Buffer in TBS, and incubated overnight at 4°C with the same primary antibodies at the same dilution as for native gels in TBS containing 0.1% Tween 20. After three 15 min washes in TTBS, membranes were incubated with secondary antibodies as above. Blots were analyzed in an Odyssey scanner.

3D modeling of GluE1 and GluE7

Models for full-length GluE1 and GluE7 were generated with RaptorX (Källberg *et al.*, 2012) based on deposited three-dimensional crystal structures of the full-length AMPA-subtype ionotropic glutamate receptor from *Rattus norvegicus*, GluA2, bound to competitive antagonists (PDB codes 4U4G (Yelshanskaya *et al.*, 2014) and 3KG2 (Sobolevsky *et al.*, 2009), respectively). Models of their respective ligand binding domains were generated with SWISS-MODEL (Biasini *et al.*, 2014) using the atomic-resolution crystal structure of the rat GluA2 LBD bound to glutamate as template (PDB code 4YU0). Model quality was assessed with MolProbity (<http://molprobity.biochem.duke.edu/>, RRID: SCR_014226). MolProbity scores for all models are given in Figure 1—source data 4. Models were inspected with MIFit (Smith, 2010) and figures were prepared with PyMOL (www.pymol.org).

Electrophysiology

Cells were visualized with an inverted epifluorescence microscope (AxioVert A.1, Zeiss) and were constantly perfused at 22–25°C with an extracellular solution containing (in mM): 145 NaCl, 2.5 KCl, 2 CaCl₂, 1 MgCl₂, 10 HEPES and 10 glucose (pH = 7.42 with NaOH; 305 mOsm/Kg). Microelectrodes were filled with an intracellular solution containing (in mM): 145 CsCl, 2.5 NaCl, 1 Cs-EGTA, 4 MgATP, 10 HEPES (pH = 7.2 with CsOH; 295 mOsm/Kg). Electrodes were fabricated from borosilicate glass (1.5 mm o.d., 1.16 i.d., Harvard Apparatus) pulled with a P-97 horizontal puller (Sutter Instruments) and polished with a forge (MF-830, Narishige) to a final resistance of 2–4 MΩ. Currents were recorded with an Axopatch 200B amplifier filtered at 1 KHz and digitized at 5 KHz using Digi-data 1440A interface with pClamp 10 software (Molecular Devices Corporation).

Whole-cell macroscopic currents were recorded from isolated or coupled pairs of mCherry or EGFP positive HEK293T cells. Rapid application (<1 ms exchange) of agonists (500 ms pulses) at a membrane potential of –60 mV was achieved by means of a theta-barrel tool (1.5 mm o.d.; Sutter Instruments) coupled to a piezoelectric translator (P-601.30; Physik Instrumente). One barrel contained extracellular solution diluted to 96% with H₂O and the other barrel contained 10 mM of the amino acid solution. For measuring current-voltage relationships, 500 ms agonist jumps were applied at different membrane voltages (–80 mV to +80 mV in 20 mV steps) and peak currents were fitted to a 5th order polynomial function. To study recovery from desensitization, a two-pulse protocol (500 ms each) was used in which a first pulse was applied followed by a second pulse at different time intervals (from 2.5 s to 25 s). The paired pulses were separated 30–60 s to allow full recovery from desensitization. To estimate the percentage of recovery, the magnitude of peak current at the second pulse (P2) was compared with the first one (P1). Electrophysiological recordings were analyzed using IGOR Pro (Wavemetrics Inc.) with NeuroMatic (Jason Rothman, UCL, RRID: SCR_004186).

Acknowledgments

We thank I Gich (Biomedical Research Institute Sant Pau) for support in biostatistics and Dr. Xavier Daura and Oscar Conchillo (Computational Biology Group and Data Center from the Institut de Biotecnologia i Biomedicina (UAB). DRV, GG, RRV, JL, PFP, and AB work at a research institute supported by the CERCA Programme/Generalitat de Catalunya.

Additional information

Funding

Funder	Grant reference number	Author
Ministerio de Economía y Competitividad	BFU2012-34398	David Ramos-Vicente Gemma Gou Rita Reig-Viader Javier Luís Àlex Bayés

Ministerio de Economía y Competitividad	BFU2015-69717-P	David Ramos-Vicente Gemma Gou Rita Reig-Viader Javier Luís Àlex Bayés
Seventh Framework Programme	304111	David Ramos-Vicente Gemma Gou Rita Reig-Viader Javier Luís Àlex Bayés
Ministerio de Economía y Competitividad	RYC-2011-08391	Àlex Bayés
Ministerio de Economía y Competitividad	RYC-2010-06210	Nerea Roher
China Scholarship Council	CSC-2013-06300075	Jie Ji
Ministerio de Economía y Competitividad	SAF2014-57994-R	Pablo Fuentes-Prior
Ministerio de Economía y Competitividad	AGL2015-65129-R	Jie Ji Nerea Roher
Generalitat de Catalunya	SGR-345-2014	David Ramos-Vicente Gemma Gou Rita Reig-Viader Javier Luís Àlex Bayés
Ministerio de Economía y Competitividad	BFU2014-57562-P	David Soto
Centre National de la Recherche Scientifique	ANR-16-CE12-0008-01	Hector Escrive
Ministerio de Economía y Competitividad	BFU2017-83317-P	David Soto
Ministerio de Economía y Competitividad	RD16/0008/0014	David Soto

The funders had no role in study design, data collection and interpretation, or the decision to submit the work for publication.

Author contributions

David Ramos-Vicente, Formal analysis, Validation, Investigation, Methodology, Writing—review and editing; Jie Ji, David Soto, Investigation, Methodology, Writing—review and editing; Esther Gratacòs-Batlle, Supervision, Investigation, Writing—review and editing; Gemma Gou, Rita Reig-Viader, Investigation, Writing—review and editing; Javier Luís, Pablo Fuentes-Prior, Formal analysis, Investigation, Methodology, Writing—review and editing; Demian Burguera, Enrique Navas-Perez, Methodology, Writing—review and editing; Jordi García-Fernández, Supervision, Methodology, Writing—review and editing; Hector Escrive, Conceptualization, Supervision, Investigation, Writing—review and editing; Nerea Roher, Funding acquisition, Investigation, Methodology, Writing—review and editing; Àlex Bayés, Conceptualization, Formal analysis, Supervision, Funding acquisition, Methodology, Writing—original draft, Project administration, Writing—review and editing

Author ORCIDs

David Ramos-Vicente  <http://orcid.org/0000-0002-2730-0850>

David Soto  <http://orcid.org/0000-0001-7995-3805>

Àlex Bayés  <http://orcid.org/0000-0002-5265-6306>

Decision letter and Author response

Decision letter <https://doi.org/10.7554/eLife.35774.119>

Author response <https://doi.org/10.7554/eLife.35774.120>

Additional files

Supplementary files

- Transparent reporting form

DOI: <https://doi.org/10.7554/eLife.35774.032>

Data availability

All data generated or analysed during this study are included in the manuscript and supporting files. Source data files have been provided for Figures 1, Figure 1 - figure supplement 1, Figure 1 - figure supplement 3, Figure 1 - figure supplement 4, Figure 2, Figure 4, Figure 4 - figure supplement 1 and Figure 4 - figure supplement 3. Genes from the sponges *Oscarella carmela*, *Sycon cilliatum* and *Leucosolenia complicata* were obtained from Compagen (<http://www.compagen.org/index.html>).

The following previously published datasets were used:

Author(s)	Year	Dataset title	Dataset URL	Database and Identifier
Sea Urchin Genome Sequencing Consortium, Sodergren E, Weinstock GM, Davidson EH, Cameron RA, Gibbs RA, Angerer RC, Angerer LM, Arnone MI, Burgess DR, Burke RD, Coffman JA, Dean M, Elphick MR, Etensohn CA, Foltz KR, Hamdoun A, Hynes RO, Klein WH, Marzluff W, McClay DR, Morris RL, Mushegian A, Rast JP, Smith LC, Thorndyke MC, Vacquier VD, Wessel GM, Wray G, Zhang L, Elsik CG, Ermolaeva O, Hlavina W, Hofmann G, Kitts P, Landrum MJ, Mackey AJ, Maglott D, Papanoulou G, Poustka AJ, Pruitt K, Sapozhnikov V, Song X, Souvorov A, Solovyev V, Wei Z, Whittaker CA, Worley K, Durbin KJ, Shen Y, Fedrigo O, Garfield D, Haygood R, Primus A, Satija R, Severson T, Gonzalez-Garay ML, Jackson AR, Milosavljevic A, Tong M, Killian CE, Livingston BT, Wilt FH, Adams N, Bellé R, Carbonneau S, Cheung R, Cormier P, Cosson B, Croce J, Fernandez-Guerra A, Genevière AM, Goel M, Kelkar H, Morales J, Mulner-	2006	The genome of the sea urchin <i>Strongylocentrotus purpuratus</i>	https://metazoa.ensembl.org/Strongylocentrotus_purpuratus/Info/Index	Ensembl Metazoa, Strongylocentrotus purpuratus

Lorillon O, Robertson AJ, Goldstone JV, Cole B, Epel D, Gold B, Hahn ME, Howard-Ashby M, Scally M, Stegeman JJ, Allgood EL, Cool J, Judkins KM, McCafferty SS, Musante AM, Obar RA, Rawson AP, Rossetti BJ, Gibbons IR, Hoffman MP, Leone A, Istrail S, Materna SC, Samanta MP, Stolc V, Tongprasit W, Tu Q, Bergeron KF, Brandhorst BP, Whittle J, Berney K, Bottjer DJ, Cales-tani C, Peterson K, Chow E, Yuan QA, Elhaik E, Graur D, Reese JT, Bosdet I, Heesun S, Marra MA, Schein J, Anderson MK, Brockton V, Buckley KM, Cohen AH, Fugmann SD, Hibino T, Loza-Coll M, Majeske AJ, Messier C, Nair SV, Pancer Z, Terwilliger DP, Agca C, Arboleda E, Chen N, Churcher AM, Hallböök F, Humphrey GW, Idris MM, Kiyama T, Liang S, Mellott D, Mu X, Murray G, Olinski RP, Raible F, Rowe M, Taylor JS, Tessmar-Raible K, Wang D, Wilson KH, Yaguchi S, Gaasterland T, Galindo BE, Gunaratne HJ, Juliano C, Kinukawa M, Moy GW, Neill AT, Nomura M, Raisch M, Reade A, Roux MM, Song JL, Su YH, Townley IK, Voronina E, Wong JL, Amore G, Branno M, Brown ER, Cavalieri V, Duboc V, Duloquin L, Flytzanis C, Gache C, Lapraz F, Lepage T, Locascio A, Martinez P, Matassi G, Matranga V, Range R, Rizzo F, Röttlinger E, Beane W, Bradham C, Byrum C, Glenn T, Hus-sain S, Manning G, Miranda E, Thomason R, Walton K,

Wikramanayke A,
Wu SY, Xu R,
Brown CT, Chen L,
Gray RF, Lee PY,
Nam J, Oliveri P,
Smith J, Muzny D,
Bell S, Chacko J,
Cree A, Curry S,
Davis C, Dinh H,
Dugan-Rocha S,
Fowler J, Gill R,
Hamilton C, Her-
nandez J, Hines S,
Hume J, Jackson L,
Jolivet A, Kovar C,
Lee S, Lewis L,
Miner G, Morgan
M, Nazareth LV,
Okwuonu G, Parker
D, Pu LL, Thorn R,
Wright R

Simakov O, Marle- taz F, Cho S-J, Edsinger-Gonzales E, Havlak P, Hell- sten U, Kuo DH, Larsson T, Lv J, Arendt D, Savage R, Osoegawa K, de Jong P, Grimwood J, Chapman JA, Shapiro H, Aerts A, Ottillar RP, Terry AY, Boore JL, Grigoriev IV, Lindberg DR, Seaver EC, Weis- blat DA, Putnam NH	2013	Insights into bilaterian evolution from three spiralian genomes	https://metazoa.ensembl.org/Lottia_gigantea/Info/Index	Ensembl Metazoa, Lottia gigantea
Chipman AD, Fer- rier DE, Brena C, Qu J, Hughes DS, Schröder R, Torres- Oliva M, Znassi N, Jiang H, Almeida FC, Alonso CR, Apostolou Z, Aqra- wi P, Arthur W, Barna JC, Blanken- burg KP, Brites D, Capella-Gutiérrez S, Coyle M, Dearden PK, Du Pasquier L, Duncan EJ, Ebert D, Eibner C, Erik- son G, Evans PD, Extavour CG, Fran- cisco L, Gabaldón T, Gillis WJ, Goodwin-Horn EA, Green JE, Griffiths- Jones S, Grimmel- khuijzen CJ, Gub- bala S, Guigó R, Han Y, Hauser F, Havlak P, Hayden L, Helbing S, Holder M, Hui JH, Hunn JP, Hunnekuhl VS, Jackson L, Javaid M, Jhangiani SN, Jiggins FM, Jones TE, Kaiser TS, Kalra D, Kenny NJ, Kor-	2014	The first myriapod genome sequence reveals conservative arthropod gene content and genome organisation in the centipede <i>Strigamia maritima</i>	https://metazoa.ensembl.org/Strigamia_maritima/Info/Index?db=core	Ensembl Metazoa, Strigamia maritima

china V, Kovar CL, Kraus FB, Lapraz F, Lee SL, Lv J, Mandapat C, Manning G, Mariotti M, Mata R, Mathew T, Neumann T, News-ham I, Ngo DN, Ninova M, Okwuonu G, Onger F, Palmer WJ, Patil S, Patraquim P, Pham C, Pu LL, Putman NH, Rabouille C, Ramos OM, Rhodes AC, Robertson HE, Robertson HM, Ronshaugen M, Rozas J, Saada N, Sánchez-Gracia A, Scherer SE, Schurko AM, Siggins KW, Simmons D, Stief A, Stolle E, Telford MJ, Tessmar-Raible K, Thornton R, van der Zee M, von Haeseler A, Williams JM, Willis JH, Wu Y, Zou X, Lawson D, Muzny DM, Worley KC, Gibbs RA, Akam M

Simakov O, Marletaz F, Cho S-J, Edsinger-Gonzales E, Havlak P, Hellsten U, Kuo DH, Larsson T, Lv J, Arendt D, Savage R, Osoegawa K, de Jong P, Grimwood J, Chapman JA, Shapiro H, Aerts A, Otiillar RP, Terry AY, Boore JL, Grigoriev IV, Lindberg DR, Seaver EC, Weisblat DA, Putnam NH	2013	Insights into bilaterian evolution from three spiralian genomes	https://metazoa.ensembl.org/Capitella_teta/Info/Index	Ensembl Metazoa, Capitella teleta
Elsik CG, Worley KC, Bennett AK, Beye M, Camara F, Childers CP, de Graaf DC, Debyser G, Deng J, Devreese B, Elhaik E, Evans JD, Foster LJ, Graur D, Guigo R; HGSC production teams, Hoff KJ, Holder ME, Hudson ME, Hunt GJ, Jiang H, Joshi V, Khetani RS, Kosarev P, Kovar CL, Ma J, Maleszka R, Moritz RF, Munoz-Torres MC, Murphy TD, Muzny DM, Newsham IF, Reese JT, Robertson HM, Robinson GE, Rueppell O,	2014	Finding the missing honey bee genes: lessons learned from a genome upgrade	https://metazoa.ensembl.org/Apis_mellifera/Info/Index	Ensembl Metazoa, Apis mellifera

Solovyev V, Stanke M, Stolle E, Tsuruda JM, Vaerenbergh MV, Waterhouse RM, Weaver DB, Whitfield CW, Wu Y, Zdobnov EM, Zhang L, Zhu D

Putnam NH, Srivastava M, Hellsten U, Dirks B, Chapman J, Salamov A, Terry A, Shapiro H, Lindquist E, Kapitonov VV, Jurka J, Genikhovich G, Grigoriev IV, Lucas SM, Steele RE, Finnerty JR, Technau U, Martindale MQ	2007	Sea anemone genome reveals ancestral eumetazoan gene repertoire and genomic organization	https://metazoa.ensembl.org/Nematostella_vectensis/Info/Index	Ensembl Metazoa, Nematostella vectensis
Srivastava M, Begovic E, Chapman J, Putnam NH, Hellsten U, Kawashima T, Kuo A, Mitros T, Salamov A, Carpenter ML, Signorovitch AY, Moreno MA, Kamm K, Grimwood J, Schmutz J, Shapiro H, Grigoriev IV, Buss LW, Schierwater B, Dellaporta SL	2008	The Trichoplax genome and the nature of placozoans	https://metazoa.ensembl.org/Trichoplax_adhaerens/Info/Index?db=core	Ensembl Metazoa, Trichoplax adhaerens
Ryan JF, Pang K, Schnitzler CE, Nguyen AD, Moreland RT, Simmons DK, Koch BJ, Francis WR, Havlak P; NISC Comparative Sequencing Program, Smith SA, Putnam NH, Haddock SH, Dunn CW, Wolfsberg TG, Mullikin JC, Martindale MQ	2013	The genome of the ctenophore Mnemiopsis leidyi and its implications for cell type evolution	https://metazoa.ensembl.org/Mnemiopsis_leidyi/Info/Index	Ensembl Metazoa, Mnemiopsis leidyi
Arabidopsis Genome Initiative	2000	Analysis of the genome sequence of the flowering plant Arabidopsis thaliana	https://www.arabidopsis.org/browse/genefamily/lonchannels.jsp	The Arabidopsis Information Resource, TAIR
Genome Reference Consortium	2017	Genome Reference Consortium Human Build 38 patch release 12 (GRCh38.p12)	https://www.ensembl.org/Homo_sapiens/Info/Index?db=core	Ensembl, Homo_sapiens
Genome Reference Consortium	2017	Genome Reference Consortium Mouse Build 38 patch release 6 (GRCm38.p6)	https://www.ensembl.org/Mus_musculus/Info/Index	Ensembl, Mus_musculus
Genome Reference Consortium	2017	Genome Reference Consortium Zebrafish Build 11	https://www.ensembl.org/Danio_erio/Info/Index	Ensembl, danio_erio
International Chicken Genome Consortium	2015	Gallus_gallus-5.0	https://www.ensembl.org/Gallus_gallus/Info/Index?db=core	Ensembl, Gallus_gallus
DOE Joint Genome Institute	2009	v4.2	https://www.ensembl.org/Xenopus_tropicalis/Info/Index	Ensembl, Xenopus 4.2

Simakov O, Kawashima T, Marlétaz F, Jenkins J, Koyanagi R, Mitros T, Hisata K, Bredeson J, Shoguchi E, Gyoja F, Yue JX, Chen YC, Freeman RM Jr, Sasaki A, Hikosaka-Katayama T, Sato A, Fujie M, Baughman KW, Levine J, Gonzalez P, Cameron C, Fritzenwanker JH, Pani AM, Goto H, Kanda M, Arakaki N, Yamasaki S, Qu J, Cree A, Ding Y, Dinh HH, Dugan S, Holder M, Jhangiani SN, Kovar CL, Lee SL, Lewis LR, Morton D, Nazareth LV, Okwuonu G, Santibanez J, Chen R, Richards S, Muzny DM, Gillis A, Peshkin L, Wu M, Humphreys T, Su YH, Putnam NH, Schmutz J, Fujiyama A, Yu JK, Tagawa K, Worley KC, Gibbs RA, Kirschner MW, Lowe CJ, Satoh N, Rokhsar DS	2015	Hemichordate genomes and deuterostome origins	https://metazome.jgi.doe.gov/pz/portal.html#!search?show=KEY-WORD&method=Org_Skowalevskii_er	Metazome, v3.2
Huang S, Chen Z, Yan X, Yu T, Huang G, Yan Q, Pontarotti PA, Zhao H, Li J, Yang P, Wang R, Li R, Tao X, Deng T, Wang Y, Li G, Zhang Q, Zhou S, You L, Yuan S, Fu Y, Wu F, Dong M, Chen S	2014	Decelerated genome evolution in modern vertebrates revealed by analysis of multiple lancelet genomes	http://genome.bucm.edu.cn/lancelet/search.php	LanceletDB, B. belcheri_HapV2(v7h2)_cds
Satou Y, Kawashima T, Shoguchi E, Nakayama A	2005	An integrated database of the ascidian, <i>Ciona intestinalis</i> : towards functional genomics	https://www.ncbi.nlm.nih.gov/genome/49	NCBI Genome, 49
Martín-Durán JM, Hejnal A	2015	The study of <i>Priapulus caudatus</i> reveals conserved molecular patterning underlying different gut morphogenesis in the Ecdysozoa	https://www.ncbi.nlm.nih.gov/genome/?term=Priapulus+caudatus	NCBI Genome, 789
Hall MR, Kocot KM, Baughman KW, Fernandez-Valverde SL, Gauthier MEA, Hatleberg WL, Krishnan A, McDougall C, Motti CA, Shoguchi E, Wang T, Xiang X, Zhao M, Bose U, Shinzato C, Hisata K, Fujie M, Kanda M, Cummins SF, Satoh N, Degnan SM, Degnan BM.	2017	The crown-of-thorns starfish genome as a guide for biocontrol of this coral reef pest	https://www.ncbi.nlm.nih.gov/genome/?term=acanthaster+planci	NCBI Genome, 7870

Simakov O, Takeshi Kawashima, Ferdinand Marletaz, Jerry Jenkins, Ryo Koyanagi, Therese Mitros, Kanako Hisata, Jessen Bredeson, Eiichi Shoguchi, Fuki Gyoja, Jia-Xing Yue, Robert Freeman, Akane Sasaki, Tomoe Hikosaka-Katayama, Atsuko Sato, Manabu Fujie, Kenneth W. Baughman, Judith Levine, Paul Gonzalez, Christopher Cameron, Jens Fritzenwanker, Ariel Pani, Hiroki Goto, Miyuki Kanda, Nana Arakaki, Shinichi Yamasaki, Jiaxin Qu, Andrew Cree, Yan Ding, Huyen H. Dinh, Shannon Dugan, Michael Holder, Shalini N. Jhangiani, Christie L. Kovar, Sandra L. Lee, Lora R. Lewis, Donna Morton, Lynne V. Nazareth, Geoffrey Okwuonu, Jireh Santibanez, Rui Chen, Stephen Richards, Donna M. Muzny, Leonid Peshkin, Michael Wu, Tom Humphreys, Yi-Hsien Su, Nicholas Putnam, Jeremy Schmutz, Asao Fujiiyama, Jr-Kai Yu, Kunifumi Tagawa, Kim C Worley, Richard A. Gibbs, Marc W. Kirschner, Christopher J Lowe, Noriyuki Satoh, Daniel S Rokhsar, John Gerhart	2015	Hemichordate genomes and deuterostome origins	http://marinegenomics.oist.jp/acornworm/viewer/info?project_id=33	Marine Genomics Unit, Ptychodera flava
Shinzato C, Shoguchi E, Kawashima T, Hamada M, Hisata K, Tanaka M, Fujie M, Fujiwara M, Koyanagi R, Ikuta T, Fujiiyama A, Miller DJ	2011	Using the <i>Acropora digitifera</i> genome to understand coral responses to environmental change	http://marinegenomics.oist.jp/coral/viewer/info?project_id=3	Marine Genomics Unit, <i>Acropora digitifera</i>
Nicholas H. Putnam, Thomas Butts, David E. K. Ferrier, Rebecca F. Furlong, Uffe Hellsten, Takeshi Kawashima, Marc Robinson-Rechavi, Eiichi Shoguchi, Astrid Terry, Jr-Kai Yu, E'lia Benito-	2008	The amphioxus genome and the evolution of the chordate karyotype	https://genome.jgi.doe.gov/Brafl1/Brafl1.home.html	Joint Genome Institute, Brafl1

Gutiérrez, Inna
 Dubchak, Jordi
 Garcia-Fernández,
 Jeremy J. Gibson-
 Brown, Igor V. Gri-
 goriev, Amy C.
 Horton, Pieter J. de
 Jong, Jerzy Jurka,
 Vladimir V. Kapito-
 nov, Yuji Kohara,
 Yoko Kuroki, Erika
 Lindquist, Susan
 Lucas, Kazutoyo
 Osoegawa, Len A.
 Pennacchio, Asaf A.
 Salamov, Yutaka
 Satou, Tatjana Sau-
 ka-Spengler, Jer-
 emy Schmutz,
 Tadasu Shin-I, At-
 sushii Toyoda, Mar-
 ianne Bronner-
 Fraser, Asao Fu-
 jiyama, Linda Z.
 Holland, Peter W.
 H. Holland, Nori
 Satoh, Daniel S.
 Rokhsar

Kim S, Martin KC	2015	Neuron-wide RNA transport combines with netrin-mediated local translation to spatially regulate the synaptic proteome	https://www.ncbi.nlm.nih.gov/genome/443	NCBI Genome, 443
Zhang G, Fang X, Guo X, Li L, Luo R, Xu F, Yang P, Zhang L, Wang X, Qi H, Xiong Z, Que H, Xie Y, Holland PW, Paps J, Zhu Y, Wu F, Chen Y, Wang J, Peng C, Meng J, Yang L, Liu J, Wen B, Zhang N, Huang Z, Zhu Q, Feng Y, Mount A, Hedgecock D, Xu Z, Liu Y, Domazet-Lošo T, Du Y, Sun X, Zhang S, Liu B, Cheng P, Jiang X, Li J, Fan D, Wang W, Fu W, Wang T, Wang B, Zhang J, Peng Z, Li Y, Li N, Chen M, He Y, Tan F, Song X, Zheng Q, Huang R, Yang H, Du X, Chen L, Yang M, Gaffney PM, Wang S, Luo L, She Z, Ming Y, Huang W, Huang B, Zhang Y, Qu T, Ni P, Miao G, Wang Q, Steinberg CE, Wang H, Qian L, Zhang G, Liu X, Yin Y	2012	The oyster genome reveals stress adaptation and complexity of shell formation	https://www.ncbi.nlm.nih.gov/genome/10758	NCBI Genome, 10758
Lim RS, Anand A, Nishimiya-Fujisawa C, Kobayashi S, Kai T	2014	Analysis of Hydra PIWI proteins and piRNAs uncover early evolutionary origins of the piRNA pathway	https://www.ncbi.nlm.nih.gov/genome/?term=Hydra+magnipapillata	NCBI Genome, 12836

Prada C, Hanna B, Budd AF, Woodley CM, Schmutz J, Grimwood J, Iglesias-Prieto R, Pandolfi JM, Levitan D, Johnson KG, Knowlton N, Kitano H, DeGiorgio M, Medina M	2016	Empty Niches after Extinctions Increase Population Sizes of Modern Corals	https://www.ncbi.nlm.nih.gov/genome/?term=orbicella+faveola	NCBI Genome, 13173
Leonid L. Moroz, Kevin M. Kocot, Mathew R. Citarella, Sohn Dosung, Tigran P. Norekian, Inna S. Povolotskaya, Anastasia P. Grigorenko, Christopher Dailey, Eugene Berezikov, Katherine M. Buckley, Andrey Ptitsyn, Denis Reshetov, Krishanu Mukherjee, Tatiana P. Moroz, Yelena Bobkova, Fahong Yu, Vladimir V. Kapitonov, Jerzy Jurka, Yuri V. Bobkov, Joshua J. Swore, David O. Girardo, Alexander Fodor, Fedor Gusev, Rachel Sanford, Rebecca Bruders, Ellen Kitter, Claudia E. Mills, Jonathan P. Rast, Romain Delle, Victor V. Solovyev, Fyodor A. Kondrashov, Billie J. Swalla, Jonathan V. Sweedler, Evgeny I. Rogae, Kenneth M. Halanynch, Andrea B. Kohn	2014	The ctenophore genome and the evolutionary origins of neural systems	https://neurobase.rc.ufl.edu/pleurobrachia	NeuroBase, pleurobrachia
Baumgarten S, Simakov O, Esherick LY, Liew YJ, Lehnert EM, Michell CT, Li Y, Hambleton EA, Guse A, Oates ME, Gough J, Weis VM, Aranda M, Pringle JR, Voolstra CR	2015	The genome of <i>Aiptasia</i> , a sea anemone model for coral symbiosis	https://www.ncbi.nlm.nih.gov/genome/?term=exaiptasia	NCBI Genome, 40858
Christian R. Voolstra, Yong Li, Yi Jin Liew, Sebastian Baumgarten, Didier Zoccola, Jean-François Flot, Sylvie Tambutté, Denis Allemand, Manuel Aranda	2017	Comparative analysis of the genomes of <i>Stylophora pistillata</i> and <i>Acropora digitifera</i> provides evidence for extensive differences between species of corals	https://www.ncbi.nlm.nih.gov/genome/?term=Acropora+digitifera	NCBI Genome, 10529
Luo YJ, Takeuchi T, Koyanagi R, Yamada L, Kanda M, Khalturina M, Fujie M, Yamasaki S,	2015	The <i>Lingula</i> genome provides insights into brachiopod evolution and the origin of phosphate biomineralization	https://www.ncbi.nlm.nih.gov/genome/?term=Lingula+anatina	NCBI Genome, 38582

Endo K, Satoh N

Simakov O, Marlettaz F, Cho SJ, Edsinger-Gonzales E, Havlak P, Hellsten U, Kuo DH, Larsson T, Lv J, Arendt D, Savage R, Osoegawa K, de Jong P, Grimwood J, Chapman JA, Shapiro H, Aerts A, Otiillar RP, Terry AY, Boore JL, Grigoriev IV, Lindberg DR, Seaver EC, Weisblat DA, Putnam NH, Rokhsar DS	2013	Insights into bilaterian evolution from three spiralian genomes	https://www.ncbi.nlm.nih.gov/genome/?term=Helobdella+robusta	NCBI Genome, 15112
Flot JF	2013	Genomic evidence for ameiotic evolution in the bdelloid rotifer <i>Adineta vaga</i>	https://www.ncbi.nlm.nih.gov/genome/?term=Adineta+vaga	NCBI Genome, 17312
Terrapon N	2014	Molecular traces of alternative social organization in a termite genome	https://www.ncbi.nlm.nih.gov/genome/?term=Zootermopsis+nevadensis	NCBI Genome, 17755
Sanggaard KW	2014	<i>Stegodyphus mimosarum</i> genome	https://www.ncbi.nlm.nih.gov/genome/?term=Stegodyphus+mimosarum	NCBI Genome, 12925
Mesquita R	2015	<i>Rhodnius prolixus</i> genome	https://www.ncbi.nlm.nih.gov/genome/?term=Rhodnius+prolixus	NCBI Genome, 447
Vicoso B, Bachtrog D	2015	Numerous transitions of sex chromosomes in Diptera	https://www.ncbi.nlm.nih.gov/genome/2619	NCBI Genome, 2619
McKenna DD	2016	<i>Anoplophora glabripennis</i> genome	https://www.ncbi.nlm.nih.gov/genome/?term=Anoplophora+glabripennis	NCBI Genome, 14033
Albertin CB, Simakov O, Mitros T, Wang ZY, Pungor JR, Edsinger-Gonzales E, Brenner S, Ragsdale CW, Rokhsar DS	2015	The octopus genome and the evolution of cephalopod neural and morphological novelties	https://metazoa.ensembl.org/Octopus_bimaculoides/Info/Index	Ensembl Metazoa, PRJNA270931

References

- Alberstein R**, Grey R, Zimmet A, Simmons DK, Mayer ML. 2015. Glycine activated ion channel subunits encoded by ctenophore glutamate receptor genes. *PNAS* **112**:E6048–E6057. DOI: <https://doi.org/10.1073/pnas.1513771112>, PMID: 26460032
- Altschul SF**, Gish W, Miller W, Myers EW, Lipman DJ. 1990. Basic local alignment search tool. *Journal of Molecular Biology* **215**:403–410. DOI: [https://doi.org/10.1016/S0022-2836\(05\)80360-2](https://doi.org/10.1016/S0022-2836(05)80360-2), PMID: 2231712
- Armstrong N**, Gouaux E. 2000. Mechanisms for activation and antagonism of an AMPA-sensitive glutamate receptor: crystal structures of the GluR2 ligand binding core. *Neuron* **28**:165–181. DOI: [https://doi.org/10.1016/S0896-6273\(00\)00094-5](https://doi.org/10.1016/S0896-6273(00)00094-5), PMID: 11086992
- Benton R**, Vannice KS, Gomez-Diaz C, Vosshall LB. 2009. Variant ionotropic glutamate receptors as chemosensory receptors in *Drosophila*. *Cell* **136**:149–162. DOI: <https://doi.org/10.1016/j.cell.2008.12.001>, PMID: 19135896
- Biasini M**, Bienert S, Waterhouse A, Arnold K, Studer G, Schmidt T, Kiefer F, Gallo Cassarino T, Bertoni M, Bordoli L, Schwede T. 2014. SWISS-MODEL: modelling protein tertiary and quaternary structure using evolutionary information. *Nucleic Acids Research* **42**:W252–W258. DOI: <https://doi.org/10.1093/nar/gku340>, PMID: 24782522
- Bowie D**, Mayer ML. 1995. Inward rectification of both AMPA and kainate subtype glutamate receptors generated by polyamine-mediated ion channel block. *Neuron* **15**:453–462. DOI: [https://doi.org/10.1016/0896-6273\(95\)90049-7](https://doi.org/10.1016/0896-6273(95)90049-7), PMID: 7646897

- Brockie PJ**, Madsen DM, Zheng Y, Mellem J, Maricq AV. 2001. Differential expression of glutamate receptor subunits in the nervous system of *Caenorhabditis elegans* and their regulation by the homeodomain protein UNC-42. *The Journal of Neuroscience* **21**:1510–1522. DOI: <https://doi.org/10.1523/JNEUROSCI.21-05-01510.2001>, PMID: 11222641
- Chiu JC**, Brenner ED, DeSalle R, Nitabach MN, Holmes TC, Coruzzi GM. 2002. Phylogenetic and expression analysis of the glutamate-receptor-like gene family in *Arabidopsis thaliana*. *Molecular Biology and Evolution* **19**:1066–1082. DOI: <https://doi.org/10.1093/oxfordjournals.molbev.a004165>, PMID: 12082126
- Conn PJ**, Pin JP. 1997. Pharmacology and functions of metabotropic glutamate receptors. *Annual Review of Pharmacology and Toxicology* **37**:205–237. DOI: <https://doi.org/10.1146/annurev.pharmtox.37.1.205>, PMID: 9131252
- Croset V**, Rytz R, Cummins SF, Budd A, Brawand D, Kaessmann H, Gibson TJ, Benton R. 2010. Ancient protostome origin of chemosensory ionotropic glutamate receptors and the evolution of insect taste and olfaction. *PLoS Genetics* **6**:e1001064. DOI: <https://doi.org/10.1371/journal.pgen.1001064>, PMID: 20808886
- Danbolt NC**. 2001. Glutamate uptake. *Progress in Neurobiology* **65**:1–105. DOI: [https://doi.org/10.1016/S0301-0082\(00\)00067-8](https://doi.org/10.1016/S0301-0082(00)00067-8), PMID: 11369436
- Darriba D**, Taboada GL, Doallo R, Posada D. 2011. ProtTest 3: fast selection of best-fit models of protein evolution. *Bioinformatics* **27**:1164–1165. DOI: <https://doi.org/10.1093/bioinformatics/btr088>, PMID: 21335321
- Dillon J**, Hopper NA, Holden-Dye L, O'Connor V. 2006. Molecular characterization of the metabotropic glutamate receptor family in *Caenorhabditis elegans*. *Biochemical Society Transactions* **34**:942–948. DOI: <https://doi.org/10.1042/BST0340942>, PMID: 17052233
- Edgar RC**. 2004. MUSCLE: a multiple sequence alignment method with reduced time and space complexity. *BMC Bioinformatics* **5**:113. DOI: <https://doi.org/10.1186/1471-2105-5-113>, PMID: 15318951
- Fonnum F**. 1984. Glutamate: a neurotransmitter in mammalian brain. *Journal of Neurochemistry* **42**:1–11. DOI: <https://doi.org/10.1111/j.1471-4159.1984.tb09689.x>, PMID: 6139418
- Furukawa H**, Singh SK, Mancusso R, Gouaux E. 2005. Subunit arrangement and function in NMDA receptors. *Nature* **438**:185–192. DOI: <https://doi.org/10.1038/nature04089>, PMID: 16281028
- Greer JB**, Khuri S, Fieber LA. 2017. Phylogenetic analysis of ionotropic L-glutamate receptor genes in the Bilateria, with special notes on *Aplysia californica*. *BMC Evolutionary Biology* **17**:11. DOI: <https://doi.org/10.1186/s12862-016-0871-1>, PMID: 28077092
- Hoang DT**, Chernomor O, von Haeseler A, Minh BQ, Vinh LS. 2018. UFBoot2: Improving the Ultrafast Bootstrap Approximation. *Molecular Biology and Evolution* **35**:518–522. DOI: <https://doi.org/10.1093/molbev/msx281>, PMID: 29077904
- Janovjak H**, Sandoz G, Isacoff EY. 2011. A modern ionotropic glutamate receptor with a K(+) selectivity signature sequence. *Nature Communications* **2**:232–235. DOI: <https://doi.org/10.1038/ncomms1231>, PMID: 21407198
- Källberg M**, Wang H, Wang S, Peng J, Wang Z, Lu H, Xu J. 2012. Template-based protein structure modeling using the RaptorX web server. *Nature Protocols* **7**:1511–1522. DOI: <https://doi.org/10.1038/nprot.2012.085>, PMID: 22814390
- Kamboj SK**, Swanson GT, Cull-Candy SG. 1995. Intracellular spermine confers rectification on rat calcium-permeable AMPA and kainate receptors. *The Journal of Physiology* **486** (Pt 2):297–303. DOI: <https://doi.org/10.1113/jphysiol.1995.sp020812>, PMID: 7473197
- Karakas E**, Furukawa H. 2014. Crystal structure of a heterotetrameric NMDA receptor ion channel. *Science* **344**:992–997. DOI: <https://doi.org/10.1126/science.1251915>, PMID: 24876489
- Kenny NJ**, Dearden PK. 2013. NMDA receptor expression and C terminus structure in the rotifer *Brachionus plicatilis* and long-term potentiation across the Metazoa. *Invertebrate Neuroscience* **13**:125–134. DOI: <https://doi.org/10.1007/s10158-013-0154-0>, PMID: 23546643
- Koh DS**, Burnashev N, Jonas P. 1995. Block of native Ca(2+)-permeable AMPA receptors in rat brain by intracellular polyamines generates double rectification. *The Journal of Physiology* **486** (Pt 2):305–312. DOI: <https://doi.org/10.1113/jphysiol.1995.sp020813>, PMID: 7473198
- Krishnan A**, Almén MS, Fredriksson R, Schiöth HB. 2013. Remarkable similarities between the hemichordate (*Saccoglossus kowalevskii*) and vertebrate GPCR repertoire. *Gene* **526**:122–133. DOI: <https://doi.org/10.1016/j.gene.2013.05.005>, PMID: 23685280
- Kristensen AS**, Hansen KB, Naur P, Olsen L, Kurtkaya NL, Dravid SM, Kvist T, Yi F, Pøhlsgaard J, Clausen RP, Gajhede M, Kastrop JS, Traynelis SF. 2016. Pharmacology and Structural Analysis of Ligand Binding to the Orthosteric Site of Glutamate-Like GluD2 Receptors. *Molecular Pharmacology* **89**:253–262. DOI: <https://doi.org/10.1124/mol.115.100909>, PMID: 26661043
- Kucharski R**, Mitri C, Grau Y, Maleszka R. 2007. Characterization of a metabotropic glutamate receptor in the honeybee (*Apis mellifera*): implications for memory formation. *Invertebrate Neuroscience* **7**:99–108. DOI: <https://doi.org/10.1007/s10158-007-0045-3>, PMID: 17372777
- Kumar J**, Schuck P, Mayer ML. 2011. Structure and assembly mechanism for heteromeric kainate receptors. *Neuron* **71**:319–331. DOI: <https://doi.org/10.1016/j.neuron.2011.05.038>, PMID: 21791290
- Kumar S**, Stecher G, Suleski M, Hedges SB. 2017. TimeTree: a resource for timelines, timetrees, and divergence times. *Molecular Biology and Evolution* **34**:1812–1819. DOI: <https://doi.org/10.1093/molbev/msx116>, PMID: 28387841
- Mayer ML**. 2005. Crystal structures of the GluR5 and GluR6 ligand binding cores: molecular mechanisms underlying kainate receptor selectivity. *Neuron* **45**:539–552. DOI: <https://doi.org/10.1016/j.neuron.2005.01.031>, PMID: 15721240

- Miller MA, Pfeiffer W, Schwartz T. 2010. Creating the CIPRES Science Gateway for inference of large phylogenetic trees. *Proceedings of the Gateway Computing Environments Workshop* **14**:1–8. DOI: <https://doi.org/10.1109/GCE.2010.5676129>
- Mitri C, Parmentier ML, Pin JP, Bockaert J, Grau Y. 2004. Divergent evolution in metabotropic glutamate receptors. A new receptor activated by an endogenous ligand different from glutamate in insects. *The Journal of Biological Chemistry* **279**:9313–9320. DOI: <https://doi.org/10.1074/jbc.M310878200>, PMID: 14660580
- Moroz LL, Kocot KM, Citarella MR, Dosung S, Norekian TP, Povolotskaya IS, Grigorenko AP, Dailey C, Berezikov E, Buckley KM, Ptitsyn A, Reshetov D, Mukherjee K, Moroz TP, Bobkova Y, Yu F, Kapitonov VV, Jurka J, Bobkov YV, Swore JJ, et al. 2014. The ctenophore genome and the evolutionary origins of neural systems. *Nature* **510**: 109–114. DOI: <https://doi.org/10.1038/nature13400>, PMID: 24847885
- Naur P, Hansen KB, Kristensen AS, Dravid SM, Pickering DS, Olsen L, Vestergaard B, Egebjerg J, Gajhede M, Traynelis SF, Kastrop JS. 2007. Ionotropic glutamate-like receptor delta2 binds D-serine and glycine. *PNAS* **104**:14116–14121. DOI: <https://doi.org/10.1073/pnas.0703718104>, PMID: 17715062
- Nguyen LT, Schmidt HA, von Haeseler A, Minh BQ. 2015. IQ-TREE: a fast and effective stochastic algorithm for estimating maximum-likelihood phylogenies. *Molecular Biology and Evolution* **32**:268–274. DOI: <https://doi.org/10.1093/molbev/msu300>, PMID: 25371430
- Nielsen H, Predicting secretory proteins with SignalP. 2017 **1611**. *Methods in Molecular Biology*. New York: Springer 59–73.
- Pascual-Anaya J, D’Aniello S. 2006. Free amino acids in the nervous system of the amphioxus *Branchiostoma lanceolatum*. A comparative study. *International Journal of Biological Sciences* **2**:87–92. DOI: <https://doi.org/10.7150/ijbs.2.87>, PMID: 16733539
- Pin JP, Galvez T, Prézeau L, Evolution PL. 2003. Evolution, structure, and activation mechanism of family 3/C G2558(03)00038-X, PMID: 12782243
- Putnam NH, Srivastava M, Hellsten U, Dirks B, Chapman J, Salamov A, Terry A, Shapiro H, Lindquist E, Kapitonov VV, Jurka J, Genikhovich G, Grigoriev IV, Lucas SM, Steele RE, Finnerty JR, Technau U, Martindale MQ, Rokhsar DS. 2007. Sea anemone genome reveals ancestral eumetazoan gene repertoire and genomic organization. *Science* **317**:86–94. DOI: <https://doi.org/10.1126/science.1139158>, PMID: 17615350
- Riesgo A, Farrar N, Windsor PJ, Giribet G, Leys SP. 2014. The analysis of eight transcriptomes from all poriferan classes reveals surprising genetic complexity in sponges. *Molecular Biology and Evolution* **31**:1102–1120. DOI: <https://doi.org/10.1093/molbev/msu057>, PMID: 24497032
- Ronquist F, Teslenko M, van der Mark P, Ayres DL, Darling A, Höhna S, Larget B, Liu L, Suchard MA, Huelsenbeck JP. 2012. MrBayes 3.2: efficient Bayesian phylogenetic inference and model choice across a large model space. *Systematic Biology* **61**:539–542. DOI: <https://doi.org/10.1093/sysbio/sys029>, PMID: 22357727
- Ryan JF, Pang K, Schnitzler CE, Nguyen AD, Moreland RT, Simmons DK, Koch BJ, Francis WR, Havlak P, Smith SA, Putnam NH, Haddock SH, Dunn CW, Wolfsberg TG, Mullikin JC, Martindale MQ, Baxevanis AD NISC Comparative Sequencing Program. 2013. The genome of the ctenophore *Mnemiopsis leidyi* and its implications for cell type evolution. *Science* **342**:1242592. DOI: <https://doi.org/10.1126/science.1242592>, PMID: 24337300
- Salussolia CL, Gan Q, Kazi R, Singh P, Allopenna J, Furukawa H, Wollmuth LP. 2013. A eukaryotic specific transmembrane segment is required for tetramerization in AMPA receptors. *Journal of Neuroscience* **33**:9840–9845. DOI: <https://doi.org/10.1523/JNEUROSCI.2626-12.2013>, PMID: 23739980
- Shinzato C, Shoguchi E, Kawashima T, Hamada M, Hisata K, Tanaka M, Fujie M, Fujiwara M, Koyanagi R, Ikuta T, Fujiyama A, Miller DJ, Satoh N. 2011. Using the *Acropora digitifera* genome to understand coral responses to environmental change. *Nature* **476**:320–323. DOI: <https://doi.org/10.1038/nature10249>, PMID: 21785439
- Simakov O, Marletaz F, Cho SJ, Edsinger-Gonzales E, Havlak P, Hellsten U, Kuo DH, Larsson T, Lv J, Arendt D, Savage R, Osoegawa K, de Jong P, Grimwood J, Chapman JA, Shapiro H, Aerts A, Otilar RP, Terry AY, Boore JL, et al. 2013. Insights into bilaterian evolution from three spiralian genomes. *Nature* **493**:526–531. DOI: <https://doi.org/10.1038/nature11696>, PMID: 23254933
- Simakov O, Kawashima T, Marlétaz F, Jenkins J, Koyanagi R, Mitros T, Hisata K, Bredeson J, Shoguchi E, Gyoja F, Yue JX, Chen YC, Freeman RM, Sasaki A, Hikosaka-Katayama T, Sato A, Fujie M, Baughman KW, Levine J, Gonzalez P, et al. 2015. Hemichordate genomes and deuterostome origins. *Nature* **527**:459–465. DOI: <https://doi.org/10.1038/nature16150>, PMID: 26580012
- Smith B. 2010. MIFit is a cross-platform interactive graphics application for molecular modeling, fitting, and refinement of protein structures from x-ray crystallography. *MIFit*. <https://github.com/mifit/mifit>
- Sobolevsky AI, Rosconi MP, Gouaux E. 2009. X-ray structure, symmetry and mechanism of an AMPA-subtype glutamate receptor. *Nature* **462**:745–756. DOI: <https://doi.org/10.1038/nature08624>, PMID: 19946266
- Tamura K, Stecher G, Peterson D, Filipksi A, Kumar S. 2013. MEGA6: Molecular evolutionary genetics analysis version 6.0. *Molecular Biology and Evolution* **30**:2725–2729. DOI: <https://doi.org/10.1093/molbev/mst197>, PMID: 24132122
- Taniura H, Sanada N, Kuramoto N, Yoneda Y. 2006. A metabotropic glutamate receptor family gene in *Dictyostelium discoideum*. *Journal of Biological Chemistry* **281**:12336–12343. DOI: <https://doi.org/10.1074/jbc.M512723200>, PMID: 16527814
- Tikhonov DB, Magazanik LG. 2009. Origin and molecular evolution of ionotropic glutamate receptors. *Neuroscience and Behavioral Physiology* **39**:763–773. DOI: <https://doi.org/10.1007/s11055-009-9195-6>, PMID: 19779829

- Traynelis SF**, Wollmuth LP, McBain CJ, Menniti FS, Vance KM, Ogden KK, Hansen KB, Yuan H, Myers SJ, Dingledine R. 2010. Glutamate receptor ion channels: structure, regulation, and function. *Pharmacological Reviews* **62**:405–496. DOI: <https://doi.org/10.1124/pr.109.002451>, PMID: 20716669
- Waterhouse AM**, Procter JB, Martin DM, Clamp M, Barton GJ. 2009. Jalview Version 2—a multiple sequence alignment editor and analysis workbench. *Bioinformatics* **25**:1189–1191. DOI: <https://doi.org/10.1093/bioinformatics/btp033>, PMID: 19151095
- Yao Y**, Harrison CB, Freddolino PL, Schulten K, Mayer ML. 2008. Molecular mechanism of ligand recognition by NR3 subtype glutamate receptors. *The EMBO Journal* **27**:2158–2170. DOI: <https://doi.org/10.1038/emboj.2008.140>, PMID: 18636091
- Yelshanskaya MV**, Li M, Sobolevsky AI. 2014. Structure of an agonist-bound ionotropic glutamate receptor. *Science*. **345**:1070–1074. DOI: <https://doi.org/10.1126/science.1256508>, PMID: 25103407